Thermochimica Acta 722 (2023) 179456

Contents lists available at ScienceDirect

Thermochimica Acta

journal homepage: www.elsevier.com/locate/tca

Heat capacity of poly(*N*-vinylpyrrolidone)

Kazuhiko Ishikiriyama [a,*], Keisuke Kondo [a], Yuji Miyazaki [b], Yuto Sasada [b], Keisuke Sawada [a], Ryo Endo [a], Naoki Man [a], Motohiro Nakano [b], Yasuhiro Nakazawa [b,c]

[a] Toray Research Center, Inc., 2-11, Sonoyama 3-chome, Shiga 520-8567, Japan
[b] Research Center for Thermal and Entropic Science, Graduate School of Science, Osaka University, Toyonaka, Osaka 560-0043, Japan
[c] Department of Chemistry, Graduate School of Science, Osaka University, Toyonaka, Osaka 560-0043, Japan

ARTICLE INFO

Keywords:
Heat capacity
Polyvinylpyrrolidone
Glass transition
Skeletal vibration
Group vibration
Deep neural network

ABSTRACT

As a first step in the analysis of the water state in biocompatible poly(*N*-vinylpyrrolidone) (PVP), the heat capacity of dried PVP was measured over a temperature range 15–520 K by adiabatic calorimetry and differential scanning calorimetry (DSC) to determine the recommended values. Based on these values, the heat capacity of the sold state was analyzed using an approximate group vibrational spectrum and skeletal vibrations. The 2-pyrrolidone-ring group vibrations of 34 modes were determined from the *ab initio* calculations based on density functional theory regarding the hydrogen-terminated dimer of PVP. The six skeletal vibrational modes are well represented by a Tarasov function with theta temperature of $\Theta_1 = 646.0$ K and $\Theta_3 = 81.9$ K, which were obtained from a three-step mesh optimization. The heat capacity of the liquid was fitted to a linear function: $C_P^{\text{liquid}} = 0.2909\ T + 101.9$ (in J K^{-1} mol^{-1}). The change in heat capacity, ΔC_P^0, of amorphous PVP at the glass transition temperature (440 K) is 29.3 J K^{-1} mol^{-1}. The values of ΔC_P^0, Θ_1 and Θ_3 agreed with the deep-learning predictions based on the ATHAS data bank with a relative error within 20%. Using the obtained characteristic parameters and group vibrations, the calculated heat capacities as a function of temperature (which correspond to the DSC baseline) were determined.

1. Introduction

Polyvinylpyrrolidone (PVP), whose repeating structural units are shown in Fig. 1, is widely used for medical material applications due to its biocompatibility. For example, PVP is added to polysulfone-hollow-fiber membranes commercialized as artificial kidneys to inhibit the adsorption of biological proteins such as platelets on the membrane surface. This suppression of the adsorption of biological proteins to the membrane surface is related to the intermediate water present in the medical material. Tanzawa et al. suggested that intermediate water in medical materials, which freezes and melts below 273.15 K, is related to biocompatibility [1,2]. In contrast, Tanaka et al. defined intermediate water as water in which cold crystallization during heating is observed in the temperature range below 273.15 K, and clarified in detail that the intermediate water is deeply related to bioinertness and hemocompatibility of medical material surfaces by using various analytical methods such as differential scanning calorimetry (DSC), X-ray diffractometry, solid state nuclear magnetic resonance, in situ attenuated total reflection infrared spectroscopy and atomic force microscopy [3–5]. In fact, intermediate water exists in the hydrous PVP [6]. However, it is still not completely clear why the intermediate water is related to biocompatibility. At least for biocompatibility, a thermodynamic analysis approach based on the heat capacity of PVP has not been implemented. Moreover, the melting point of water in hydrous PVP is distributed over a wide temperature range, and hence the temperature range of the broad phase transition must be accurately determined in order to analyze the state of water in hydrous polymers: free water (bulk water), intermediate water, and nonfreezing water. However, since DSC measurements alone cannot determine the heat-flow baseline, a precise analysis based on heat capacity is essential. Unfortunately, the heat capacity of PVP is not yet registered in the Advanced Thermal Analysis System (ATHAS) data bank built by Wunderlich et al. [7–12], where polymer-specific thermal properties are collected. Furushima et al. has reported the heat capacity of neat PVP over a temperature range of 403–468 K [6], but it has not been measured over a wide enough temperature range for detailed analysis. Franks and Wakabayashi also measured the heat capacity of aqueous PVP solutions using DSC and attempted a thermodynamic analysis of the folding and unfolding conformations of the protein based

* Corresponding author.
E-mail address: kazuhiko.ishikiriyama.s8@trc.toray (K. Ishikiriyama).

https://doi.org/10.1016/j.tca.2023.179456
Received 2 November 2022; Received in revised form 31 January 2023; Accepted 1 February 2023
Available online 11 February 2023

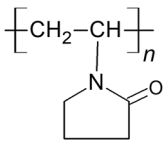

Fig. 1. Structure of the repeating unit of poly(*N*-vinylpyrrolidone) (PVP).

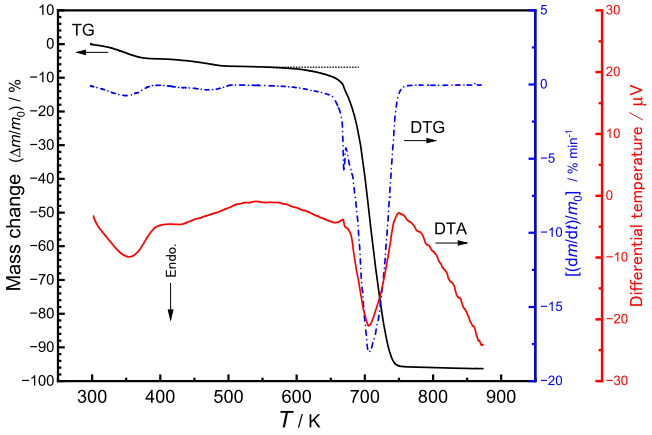

Fig. 2. Typical TG-DTA curves for the as-received PVP.

on the N- and D-states, because chemically its side chains resemble a proline; however, the analysis has not been conducted separately for the three aforementioned states of water [13]. Therefore, as a first step to elucidate the intermediate water, we measured the temperature dependence of the heat capacity of PVP in the dry state using adiabatic calorimetry and DSC to obtain the recommended values of heat capacity and then analyzed these values. The thermal properties of PVP were then predicted by deep learning based on the ATHAS data bank and compared with the experimental data obtained in this study in order to confirm the validity of both methods.

2. Heat capacity analysis method for polymers

2.1. Heat capacity at constant volume based on the group vibrations of the solid polymer

The heat capacity of solid polymers can be calculated based on group and skeletal vibrations. The analysis procedure described below has already been established by Wunderlich et al. [7–10]. Although the constant-pressure heat capacity (C_P^{exp}) can be obtained by measurement, the constant-volume heat capacity (C_V^{exp}) is more suitable for analysis. Thus, C_P^{exp} is first converted to C_V^{exp} using the following approximation:

$$C_V^{exp} = C_P^{exp} - 3RA_0' C_P T/T_m^0 \quad (1)$$

where R is the gas constant, A'_0 is the approximate universal constant with a value of 3.9×10^{-3} K mol J^{-1} and T_m^0 is the equilibrium melting point. C_V^{exp} consists of the sum of the group vibration contribution (C_V^{group}) and the skeletal vibration contribution ($C_V^{skeletal}$). The former (C_V^{group}) is calculated from the following equation:

$$C_V^{group} = \sum C_V^{Einstein} + \sum C_V^{box} \quad (2)$$

The first term in Eq. (2) is related to the contribution to the heat capacity at constant volume in one mole of harmonic oscillator with frequency ν, and is obtained from Eq. (3):

$$C_V^{Einstein}/N_E R = E(\theta_E/T) \quad (3)$$

where N_E is the number operator of the harmonic oscillator, θ_E (= $h\nu/k$, where h is Planck's constant and k is Boltzmann's constant) is the characteristic temperature (K), which is the wavenumber (cm^{-1}) multiplied by 1.4388 cm K, and $\boldsymbol{E}(\theta/T)$ is the Einstein function, as shown in the following equation:

$$\boldsymbol{E}(\theta/T) = (\theta/T)^2 e^{\theta/T} \Big/ \left(e^{\theta/T} - 1\right)^2 \quad (4)$$

The second term in Eq. (2) is related to the contribution to the heat capacity at constant volume in the group vibrations that spread over a wider frequency range approximated by box-distributions, and is obtained from the following equation:

$$C_V^{box} \Big/ N_B R = \frac{\theta_U}{\theta_U - \theta_L}\left[\boldsymbol{D}_1\left(\frac{\theta_U}{T}\right) - \frac{\theta_L}{\theta_U}\boldsymbol{D}_1\left(\frac{\theta_L}{T}\right)\right] \quad (5)$$

where N_B is the number of vibrators for the box distribution and $\boldsymbol{D}_1(\theta/T)$ is the one-dimensional Debye function (described later). θ_L (= $h\nu_L/k$) and θ_U(= $h\nu_U/k$) are the characteristic temperatures of the box distribution for the lower frequency (ν_L) and upper frequency (ν_U), respectively.

Thus, C_V^{group} is approximated using the Einstein and box distribution functions. Although the spectrum due to its group vibrations is a considerable simplification compared to the actual molecular vibration spectrum, it has been found that the approximation explains well the measured heat capacity of polymers [10].

2.2. Heat capacity at constant volume based on the skeletal vibrations of the solid polymer

Once C_V^{group} is obtained, $C_V^{skeletal\text{-}exp}$ is computed from the following equation:

$$C_V^{skeletal-exp} = C_V^{exp} - C_V^{group} \quad (6)$$

In addition, $C_V^{skeletal\text{-}cal}$ is calculated by using the general Tarasov function:

$$\begin{aligned} C_V^{skeletal-cal}/N_S R &= \boldsymbol{T}(\Theta_1/T,\ \Theta_2/T, \Theta_3/T) \\ &= \boldsymbol{D}_1(\Theta_1/T) - (\Theta_2/\Theta_1)[\boldsymbol{D}_1(\Theta_2/T) - \boldsymbol{D}_2(\Theta_2/T)] \\ &\quad -\left(\Theta_3^2/(\Theta_1\Theta_2)\right)[\boldsymbol{D}_2(\Theta_3/T) - \boldsymbol{D}_3(\Theta_3/T)] \end{aligned} \quad (7)$$

where N_s is the number of skeletal vibrators, Θ_1, Θ_2 and Θ_3 are the three characteristic parameters and the functions labeled $\boldsymbol{D}_1$, $\boldsymbol{D}_2$ and $\boldsymbol{D}_3$ are the one-, two- and three-dimensional Debye functions:

$$\boldsymbol{D}_i(\Theta_i/T) = i(T/\Theta_i)^i \int_0^{\Theta_i/T} \frac{(\Theta/T)^{i+1} e^{\Theta_i/T}}{\left[e^{(\Theta/T)} - 1\right]^2} d(\Theta/T) \quad (8)$$

where i is equal to 1, 2, or 3. $C_V^{skeletal\text{-}exp}$ is fitted to the general Tarasov function with the three characteristic parameters Θ_1, Θ_2 and Θ_3 in polymers such as starch with a planar structure [14]. In linear macromolecules that have no contribution from a planar structure, Θ_2 becomes equal to Θ_3 and Eq. (7) is reduced to the following equation:

$$C_V^{skeletal-cal}/N_S R = \boldsymbol{D}_1(\Theta_1/T) - (\Theta_3/\Theta_1)[\boldsymbol{D}_1(\Theta_3/T) - \boldsymbol{D}_3(\Theta_3/T)] \quad (9)$$

This equation was originally proposed by Tarasov and applied to data sets on linear macromolecules [7,10]. $C_V^{skeletal\text{-}cal}$ can thus be computed using the one- and three-dimensional Debye functions regarding intra- and intermolecular interactions, respectively. Both Debye functions are approximately obtained by numerical calculations [15].

The unknown characteristic parameters Θ_1, Θ_2 and Θ_3 are determined from the minimum of the root mean square error (RMSE) between $C_V^{skeletal\text{-}exp}$ and $C_V^{skeletal\text{-}cal}$:

Table 1
Heat capacities of anhydrous solid PVP[a].

T / K	$C_p^{adiabatic}$ [b] / J K^{-1} mol^{-1}	C_P^{DSC} [c] / J K^{-1} mol^{-1}	$C_P^{recommended}$ / J K^{-1} mol^{-1}	C_P^{cal} / J K^{-1} mol^{-1}	Index[d]	T / K	$C_p^{adiabatic}$ [b] / J K^{-1} mol^{-1}	C_P^{DSC} [c] / J K^{-1} mol^{-1}	$C_P^{recommended}$ / J K^{-1} mol^{-1}	C_P^{cal} / J K^{-1} mol^{-1}	Index[d]
15	5.87	NA	5.87	5.87	1	300	135.17	134.9	135.0	137.3	2
20	9.63	NA	9.63	9.81	1	310	138.92	139.3	139.1	141.8	2
25	13.58	NA	13.58	13.54	1	320	143.48	143.6	143.6	146.4	2
30	17.50	NA	17.50	17.08	1	330	147.86	148.1	148.0	150.9	2
40	24.73	NA	24.73	23.88	1	340	NA	152.4	152.4	155.4	3
50	31.34	NA	31.34	30.42	1	350	NA	156.9	156.9	160.0	3
60	37.40	NA	37.40	36.60	1	360	NA	161.6	161.6	164.5	3
70	42.88	NA	42.88	42.30	1	370	NA	166.4	166.4	169.0	3
80	47.94	NA	47.94	47.53	1	380	NA	171.1	171.1	173.5	3
90	52.59	NA	52.59	52.34	1	390	NA	176.0	176.0	178.0	3
100	56.52	NA	56.52	56.80	1	400	NA	180.8	180.8	182.4	3
110	60.79	NA	60.79	60.99	1	410	NA	185.5	185.5	186.8	3
120	64.76	NA	64.76	64.97	1	420	NA	190.1	190.1	191.1	3
130	68.69	NA	68.69	68.82	1	430	NA	196.2	196.2	195.4	3
140	72.67	NA	72.67	72.59	1	440	NA	NA	NA	199.7	4
150	76.18	NA	76.18	76.30	1	450	NA	NA	NA	203.9	4
160	79.83	NA	79.83	80.00	1	460	NA	NA	NA	208.1	4
170	83.56	NA	83.56	83.71	1	470	NA	NA	NA	212.2	4
180	87.55	NA	87.55	87.45	1	480	NA	NA	NA	216.3	4
190	91.10	NA	91.10	91.24	1	490	NA	NA	NA	220.3	4
200	94.65	NA	94.65	95.10	1	500	NA	NA	NA	224.2	4
210	98.37	99.02	98.37	99.01	1	510	NA	NA	NA	228.1	4
220	102.6	102.8	102.6	103.0	1	520	NA	NA	NA	232.0	4
230	106.7	106.5	106.7	107.1	1	530	NA	NA	NA	235.8	4
240	110.4	110.3	110.3	111.2	2	540	NA	NA	NA	239.5	4
250	114.7	114.2	114.4	115.4	2	550	NA	NA	NA	243.2	4
260	118.7	118.3	118.5	119.7	2	560	NA	NA	NA	246.9	4
270	122.33	122.3	122.3	124.0	2	570	NA	NA	NA	250.5	4
273.15	123.50	123.6	123.6	125.4	2	580	NA	NA	NA	254.0	4
280	126.29	126.4	126.4	128.4	2	590	NA	NA	NA	257.5	4
290	130.96	130.6	130.8	132.9	2	600	NA	NA	NA	261.0	4
298.15	134.30	134.1	134.2	136.5	2						

[a] A value of 111.14 g mol^{-1} was used as the molar mass of the repeating structural unit of PVP. Solid PVP was in the glassy state.
[b] $C_P^{adiabatic}$ represents the heat capacity for anhydrous solid PVP. The CPadiabatic values were calculated by smoothing the raw data in Tables 11 and 12 using the cubic spline functions and then subtracting the effect of residual moisture. The raw data in Tables 11 and 12 were measured by adiabatic calorimetry at 297.65 K and an atmospheric pressure of 100.94 ± 0.05 kPa, and at 298.95 K and an atmospheric pressure of 99.44 ± 0.09 kPa, respectively, in a calorimeter that was filled with helium and then sealed.
[c] C_P^{DSC} represents the experimental data measured by DSC at an atmospheric pressure of 100.25 ± 0.07 kPa. Raw data are listed in Table 13.
[d] 1. Recommended experimental value ($C_P^{recommended}$) is based on the experimental data measured by adiabatic calorimetry, and the calculated heat capacity (C_P^{cal}) is obtained using Θ_1 and Θ_3, to agree with the recommended experimental data ($C_P^{recommended}$), as described in text. 2. The recommended value is the arithmetic mean between adiabatic and DSC results. 3. Recommended experimental value is based on the experimental data measured by DSC. 4. The calculated heat capacity was obtained using Θ_1 and Θ_3, because data during and above the glass transition for solid PVP are not available.

$$\mathrm{RMSE} = \sqrt{\sum_{i=1}^{n} \left(C_V^{\mathrm{skeletal-exp}} - C_V^{\mathrm{skeletal-cal}}\right)^2 \Big/ n} \tag{10}$$

where n is the number of the data. The computer programs were developed in FORTRAN [8,16], C [15] and Mathematica [17], and an efficient method for determining the characteristic parameters has been proposed [8,18]. By substituting the determined characteristic parameters Θ_1, Θ_2 and Θ_3 into either Eq. (7) or Eq. (9), $C_V^{\mathrm{skeletal\text{-}cal}}$ is calculated and then C_V^{cal} can be obtained from the following equation:

$$C_V^{cal} = C_V^{\mathrm{skeletal-cal}} + C_V^{group} \tag{11}$$

2.3. Calculated heat capacity at constant pressure from conversion of the heat capacity at constant volume

C_V^{cal} determined from Eq. (11) is then converted to C_P^{cal} using the following equation:

$$C_P^{cal} = C_V^{cal} + 3RA_0' C_P T / T_m^0 \tag{12}$$

Once the heat capacity is obtained, the temperature dependence of enthalpy (H), entropy (S), and Gibbs energy (G) can also be calculated as described later [10].

3. Experimental

3.1. Materials and preparation

The powder form of PVP (CAS: 9003-39-8) was purchased from Sigma–Aldrich (Lot # STBJ3834, 234257) and the nominal weight-average molecular weight (M_w) is about 29,000 g mol^{-1}, which was estimated from a K value of 22.6−26.7. No impurity peaks were observed in the gel permeation chromatograph-multi angle light scattering (GPC-MALS) measurement. The polymer was used without further purification. Since PVP is hygroscopic, it was heated at 373 K for 30 min and then further heated at 473 K for 10 min before heat capacity measurement.

3.2. Instrumentation

3.2.1. Adiabatic calorimetry

The heat capacities of dried PVP were measured between 15 and 330 K with a laboratory-made adiabatic microcalorimeter, which is described elsewhere [23]. The mass of the sample used was 1.13969 g. The sample was sealed in a gold-plated calorimeter cell (3 cm^3 volume) together with helium gas at atmospheric pressure to facilitate thermal contact between the sample and the cell. Buoyancy correction was made to obtain the true sample mass using the density of PVP (1.26 g cm^{-3})

Table 2
Heat capacities[a] of anhydrous liquid PVP.

T / K	C_P^{DSC} [b] / J K^{-1} mol^{-1}	$C_P^{recommended}$ [c] / J K^{-1} mol^{-1}	C_p^{cal} [d] / J K^{-1} mol^{-1}	Index [e]
430.0	NA	NA	227.0	1
440.0	NA	NA	229.9	1
450.0	NA	NA	232.8	1
460.0	235.4	235.4	235.7	2
470.0	237.5	237.5	238.6	2
480.0	240.7	240.7	241.5	2
490.0	243.9	243.9	244.4	2
500.0	246.3	246.3	247.3	2
510.0	249.6	249.6	250.2	2
520.0	253.2	253.2	253.1	2
530.0	NA	NA	256.0	3
540.0	NA	NA	259.0	3
550.0	NA	NA	261.9	3
560.0	NA	NA	264.8	3
570.0	NA	NA	267.7	3
580.0	NA	NA	270.6	3
590.0	NA	NA	273.5	3
600.0	NA	NA	276.4	3

[a] A value of 111.14 g mol^{-1} was used as the molar mass of the repeating structural unit of PVP.
[b] All the experimental data (C_P^{DSC}) were measured with DSC at an atmospheric pressure of 100.25 ± 0.07 kPa.
[c] $C_P^{recommended}$ is the recommended experimental value.
[d] C_P^{cal} is calculated from a linear function of 0.2909 ·T + 101.9 (in J K^{-1} mol^{-1}).
[e] 1. The experimental heat capacity of the liquid could not be obtained due to the glass transition. 2. $C_P^{recommended}$ is based on the experimental data measured with the present DSC data. 3. The heat capacity was not measured.

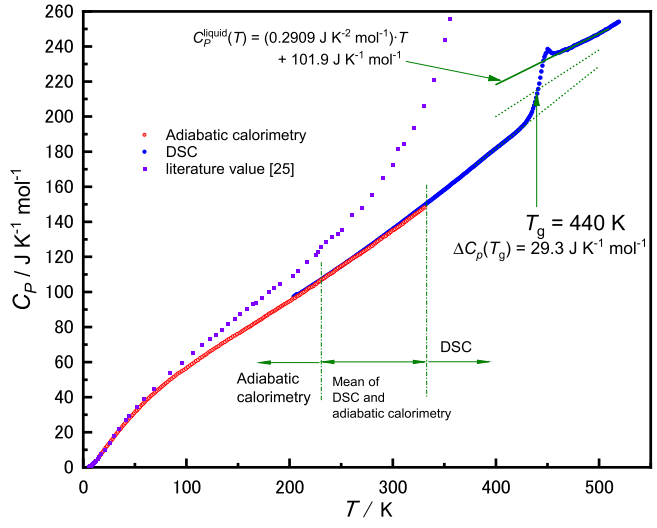

Fig. 3. Heat capacities of polyvinylpyrrolidone (PVP). Open red circles represent the results by adiabatic calorimetry, which were measured and superimposed by three runs. Closed blue circles indicate the DSC results, which are averages over three runs or more runs. Closed purple squares indicate the literature values reported by Lebedev et al. [25].

[19] and the density of air at 50% relative humidity. Without buoyancy correction, the mass of the sample would be estimated as about 0.1% less in this experimental condition, resulting in a heat capacity estimate about 0.1% higher. The thermometry was performed by a temperature transfer system using chromel–constantan thermocouples and a Rh–Fe alloy resistance thermometer (nominal 27 W; Oxford Instruments) calibrated from 1.5 to 380 K on a basis of the ITS-90 temperature scale. The resolution of the thermometry was ± 0.3 mK at 15 K and ± 0.06 mK at 80 K [20], and the inaccuracy of the calibrated temperature was ± 0.36% at 4.2 K, ± 0.030% at 100 K and ± 0.012% at 300 K. The inaccuracy of the heat capacity measurement was 1% for T < 30 K, 0.5% for 30 K < T < 60 K and 0.3% for T > 60 K. The samples were dried before measurement and set in the calorimeter cell, but because PVP is highly hygroscopic it could not be completely dried out. Furthermore, preheat treatment of the sample at 520 K prior to the heat capacity measurement could not be performed in the adiabatic calorimeter due to the system configuration of the calorimeter. Thus, the effect of residual moisture was corrected using the measured heat capacity values of the absorbed water in PVP.

3.2.2. *Differential scanning calorimetry*

A differential scanning calorimeter (DSC 8500; Perkin-Elmer) equipped with an IntracoolerII was used for the heat capacity measurement. Dry nitrogen gas was purged through the DSC cell at a flow rate of 20 mL min^{-1}. Temperature calibration was carried out to ± 0.1 K using onsets of the transition peaks for octane (216.3 K) [21], water (273.15 K) [22], indium (429.75 K) [23] and tin (505.07 K) [23]. The runs for the heat capacity of PVP, sapphire and empty baseline were carried out over a temperature range of 198–520 K at a heating rate of 10 K min^{-1}. The initial and final isotherms were 3 min. A PVP sample of about 23–44 mg and a sapphire of about 42 mg were used. The relative expanded uncertainty (coverage factor: k = 2) of the heat capacity determined using power-compensated DSC is reported to be 1.5% at 523 K [24].

As PVP has strong hygroscopic properties, the preheat-treated PVP described in Section 3.1 was set in a DSC pan in a glove box filled with an inert atmosphere of nitrogen, with a dew point of 220 K or less. The samples were further heated in the DSC cell from room temperature to 520 K at 10 K min^{-1}, dehydrated by holding at 520 K for 1 min and then cooled to 198 K at 10 K min^{-1} before starting the heat capacity measurements.

Mass determinations were done using an MX5 electro-balance (Mettler-Toledo) with a sensitivity of 1.0 mg. Data on three or more runs were averaged. Before and after each DSC measurement of PVP, the sample masses were determined. A weight loss of 1–1.5% of PVP was observed, which was attributed to water evaporation by Thermogravimetry-Mass spectroscopy (TG-MS) measurement. Thus, the sample weight after measurement was used to calculate the heat capacity of PVP.

3.2.3. *Thermogravimetry–differential thermal analysis*

The thermal stability of as-received PVP was confirmed using thermogravimetry–differential thermal analysis (TG-DTA) with a simultaneous thermogravimetric analyzer (TG-DTA STA7200RV; Hitachi High-Tech Science). Temperature calibration was carried out using onsets of the melting temperatures of tin, lead, zinc and aluminum. Dry nitrogen gas was purged at a flow rate of 200 mL min^{-1}. The TG-DTA measurement for a 10.0 mg sample, weighed into an aluminum pan, was carried out over a temperature range of 298–873 K at a heating rate of 10 K min^{-1}.

4. Results

Fig. 2 shows the TG-DTA curve of as-received PVP. When the sample is heated, two weight loss steps are observed from room temperature to 500 K and another weight loss is observed above 580 K. The former two-step weight loss would be due to desorption of surface-bound water and strongly bound water, respectively, whereas the latter would be due to thermal degradation of PVP. These results indicate that heating to 520 K removes volatile components in PVP and that heat capacity measurement is possible at least below 520 K without the influence of pyrolysis. However, above 580 K, heat capacity measurement is expected to be difficult due to thermal degradation of PVP. Heat capacity measurement in the temperature range of 520–580 K may be possible by using a quasi-isothermal method with temperature-modulated DSC.

Table 3
Contribution of methylene and CH_2CH groups to the vibrations of PVP.

Vibration types	Assignment	Number of group vibrations	Characteristic temperature [a]			Origin
			K			
Methylene group	CH_2 asymmetrical strech	1.00	θ_E	4148		Polyethylene
	CH_2 symmetrical strech	1.00	θ_E	4098		Polyethylene
	CH_2 bend	1.00	θ_E	2075		Polyethylene
	CH_2 wag	0.65	θ_L, θ_U	1698	1977	Polyethylene
	CH_2 wag	0.35	θ_E	1977		Polyethylene
	CH_2 twist and rock	0.48	θ_L, θ_U	1690	1874	Polyethylene
	CH_2 twist and rock	0.52	θ_E	1874		Polyethylene
	CH_2 rock and twist	0.04	θ_E	1494		Polyethylene
	CH_2 rock and twist	0.59	θ_L, θ_U	1038	1494	Polyethylene
	CH_2 rock and twist	0.37	θ_E	1079		Polyethylene
[$CH_2CH(R)$-] group	CH_2-CH chain strech	0.16	θ_E	1685		Polypropylene
	CH_2-CH chain strech	0.84	θ_L, θ_U	1650	1685	Polypropylene
	CH_2-CH chain strech	0.17	θ_E	1197		Polypropylene
	CH_2-CH chain strech	0.55	θ_L, θ_U	1167	1198	Polypropylene
	CH_2-CH chain strech	0.28	θ_E	1167		Polypropylene
	CH strech	1.00	θ_E	4181		Polypropylene
	CH bend	0.42	θ_L, θ_U	1963	1973	Polypropylene
	CH bend	0.58	θ_E	1966		Polypropylene
	CH bend	0.64	θ_E	1944		Polypropylene
	CH bend	0.28	θ_L, θ_U	1916	1944	Polypropylene
	CH bend	0.08	θ_E	1916		Polypropylene

[a] θ_E is the characteristic temperature for the Einstein function in Eq. (3) and θ_L and θ_U are the characteristic lower and upper temperatures for the box distribution in Eq. (5), respectively.

The results of the heat capacity measurements as a function of temperature for the solid and liquid PVP are summarized in Tables 1 and 2 and the data are illustrated in Fig. 3. These values were obtained per mol using a formula weight of 111.14 g mol^{-1} for the repeating structural unit of PVP. The data measured using adiabatic calorimetry are indicated by open circles in Fig. 3, whereas the DSC data are shown as filled circles, which are averages over three runs. The standard deviations of the multiple runs with DSC were 1.09 for 210–250 K, 1.30 for 260–350 K and 1.79 for 460–520 K.

The glass transition temperature (T_g) of PVP is determined to be 440 K (see Fig. 3). The heat capacities measured by adiabatic calorimetry ($C_P^{adiabatic}$) agree with the heat capacities measured by DSC (C_P^{DSC}) within a relative error of ±0.4% for 240–330 K, as can be seen from Table 1. In the DSC measurement, the sample weight is lower than in the adiabatic calorimetry, resulting in a larger measurement error due to the lower heat flow intensity in the low temperature range. In contrast, adiabatic calorimetry has a larger measurement error in the high temperature range due to the difficulty of adiabatic control. Considering these equipment characteristics, the recommended heat capacity values for PVP were determined by comparing the heat capacities obtained by adiabatic calorimetry and DSC. We adopted the results of adiabatic calorimetry below 230 K, the arithmetic mean of $C_P^{adiabatic}$ and C_P^{DSC} for 240–330 K and the results of DSC above 340 K as the recommended values of the heat capacity ($C_P^{recommended}$) of solid PVP. The $C_P^{recommended}$ values thus determined are summarized in Table 1.

Kulagina and Lebedev reported the heat capacity of anhydrous PVP in the temperature range 0−450 K [25] and the results are shown in Fig. 3 as closed squares. They reported T_g = 352 K for anhydrous PVP, which is 88 K lower than the T_g measured in this study. Thus, assuming that the T_g of PVP decreased from 440 K to 352 K due to the plasticizing effect of residual water, the residual water contents were calculated from the two equations introduced by Couchman [26] as follows:

$$\ln T_g^{mix} = \left[x\Delta C_P^{PVP} \ln T_g^{PVP} + (1-x)\Delta C_P^{water} \ln T_g^{water}\right] \Big/ \left(x\Delta C_P^{PVP} + (1-x)\Delta C_P^{water}\right) \quad (13)$$

$$T_g^{mix} = \left[x\,\Delta C_P^{PVP}\, T_g^{PVP} + (1-x)\Delta C_P^{water}\, T_g^{water}\right] \Big/ \left(x\Delta C_P^{PVP} + (1-x)\Delta C_P^{water}\right) \quad (14)$$

where T_g^{PVP}, T_g^{water} and T_g^{mix} are the glass transition temperatures (in K) of PVP, water and a PVP/water mixture, respectively; ΔC_P^{PVP} and ΔC_P^{water} are the heat capacity differences of PVP at T_g (in J K^{-1} g^{-1}) and of water (in J K^{-1} g^{-1}), respectively; and x is the remaining water content (in wt %). Substituting T_g = 135 K and ΔC_P^{water} = 1.94 J K^{-1} g^{-1} for water, as reported by Seki et al. [27] and T_g = 440 K and ΔC_P^{PVP} = 0.264 J K^{-1} g^{-1} for PVP, obtained in this study, residual water contents of 3 wt% from Eq. (13) and 5 wt% from Eq. (14) were obtained. Lebedev et al. measured the heat capacity after 3 hours of heat treatment at 420 K in a vacuum, but due to heat treatment below the T_g for dried PVP, a water content of 3−5 wt% remained, resulting in a T_g of 352 K for PVP, which would have resulted in higher heat capacity values. In addition, the TG (shown in Fig. 2) indicates a weight loss of 2.0 wt% at 400−520 K, before and after the T_g. Water is detected by TG-MS in this temperature range, and when PVP is allowed to absorb moisture after annealing at 520 K, weight loss is again observed in this temperature range. Therefore, the above weight loss of 2.0 wt% is attributed to water desorption. As it has been reported that water can be completely removed by heating polymeric materials to above the T_g or above the melting temperature [28], it must have been difficult to remove adsorbed water in PVP by heat treatment below the T_g.

Kulagina and Lebedev also reported the heat capacity and thermodynamic functions of *N*-vinylpyrrolidone (the monomer of PVP) at 0−330 K [29], and the heat capacities are rather closer to the literature values of PVP [25] than the values obtained in this study. However, the heat capacities of the polymer and the monomer are not necessarily close. As shown in Eq. (11), the heat capacity of an organic solid depends on the skeletal and group vibrations. Since the skeletal and group vibrations are completely different for the polymer and the monomer, their heat capacities would be different.

With regard to the heat capacity of PVP in the liquid state, as measured by DSC, the C_P^{DSC} was determined from the arithmetic mean of the heat capacities obtained from three or more measurements, which are shown in Table 2. These values were adopted as the $C_P^{recommended}$ data. In general, it is known that a linear relationship is established for the temperature dependence of the heat capacity of polymers in the liquid state [10]. For example, a linear temperature dependence of heat capacity in the liquid state is observed for aliphatic nylons [30], aliphatic polyesters [30] and aliphatic polyoxides [31]. As shown in Fig. 3, a linear temperature dependence is also observed for the heat capacity of PVP in the liquid state above the glass transition, and the

Table 4
Contribution of 2-pyrrolidone group to the vibrations of PVP obtained from *ab initio* calculation.

Vibration types	Assignment	Number of group vibrations	Characteristic temperature [a]		
				K	
pyrrolidone group	Pyrrolidone ring out-of-plane twist	1.0	θ_E	52	
	Pyrrolidone ring out-of-plane wag	1.0	θ_L, θ_U	98	121
	NCC, CCC symmetrical out-of-plane wag	1.0	θ_E	208	
	CCC symmetrical out-of-plane wag	1.0	θ_E	238	
	CNC symmetrical out-of-plane wag	1.0	θ_L, θ_U	290	341
	O=CC symmetrical in-plane scissor and rock	1.0	θ_L, θ_U	678	787
	CH_2 asymmetrical in-plane rock	1.0	θ_L, θ_U	818	835
	NCC symmetrical in-plane scissor, CC strech	1.0	θ_L, θ_U	855	914
	CCC symmetrical in-plane scissor	1.0	θ_E	944	
	CH_2 asymmetrical in-plane rock	1.0	θ_E	1062	
	CH_2 asymmetrical in-plane rock	1.0	θ_E	1235	
	CH_2 asymmetrical twist and rock	1.0	θ_E	1311	
	CC symmetrical strech	1.0	θ_E	1346	
	CC strech and CH_2 wag twist rock	1.0	θ_L, θ_U	1460	1559
	CC symmetrical strech	1.0	θ_E	1477	
	CH_2 asymmetrical twist and rock	1.0	θ_E	1574	
	CH_2 asymmetrical twist and rock	1.0	θ_E	1698	
	CH_2 asymmetrical twist and rock	1.0	θ_L, θ_U	1723	1761
	CN strech, CH_2 twist and wag	1.0	θ_E	1772	
	CH_2 symmetrical twist	1.0	θ_L, θ_U	1797	1815
	CH_2 twist and wag, CN strech	1.0	θ_E	1867	
	CH_2 twist and wag	1.0	θ_E	1889	
	CH_2 symmetrical out-of-plane wag	1.0	θ_E	1937	
	CH_2 twist and wag	1.0	θ_E	2087	
	CH_2 symmetrical in-plane scissor	1.0	θ_E	2123	
	CH_2 symmetrical in-plane scissor	1.0	θ_E	2168	
	CH_2 symmetrical in-plane scissor	1.0	θ_E	2218	
	C=O strech	1.0	θ_E	2502	
	CH_2 symmetrical strech	1.0	θ_L, θ_U	4271	4300
	CH_2 symmetrical strech	1.0	θ_E	4365	
	CH_2 symmetrical strech	1.0	θ_E	4387	
	CH_2 asymmetrical strech	1.0	θ_L, θ_U	4411	4445
	CH_2 asymmetrical strech	1.0	θ_E	4454	
	CH_2 asymmetrical strech	1.0	θ_E	4469	

[a] θ_E is the characteristic temperature for the Einstein function in Eq. (3) and θ_L and θ_U are the characteristic lower and upper temperatures for the box distribution in Eq. (5), respectively.

Table 5
Vibrational frequencies of PVP.

Assignment	Number of group vibrations
Contribution from CH_2 of main chain	
CH_2 asymmetrical strech	1
CH_2 symmetrical strech	1
CH_2 bend	1
CH_2 wag	1
CH_2 twist and rock	1
CH_2 rock and twist	1
Contribution from [$CH_2CH(R)$-] group	
CH_2-CH chain strech	2
CH strech	1
CH bend	2
Contribution from pyrrolidone group	
Pyrrolidone twist and wag	2
CCC, NCC wag	3
O=CC scissor and rock	1
CH_2 rock	3
CCC, NCC scissor	2
CH2 twist and rock	4
CC strech	3
CN strech	3
CH_2 twist wag	3
CH_2 scissor	3
C=O strech	1
CH_2 symmetrical strech	3
CH_2 asymmetrical strech	3
Skeletal vibrations	6
Total	51

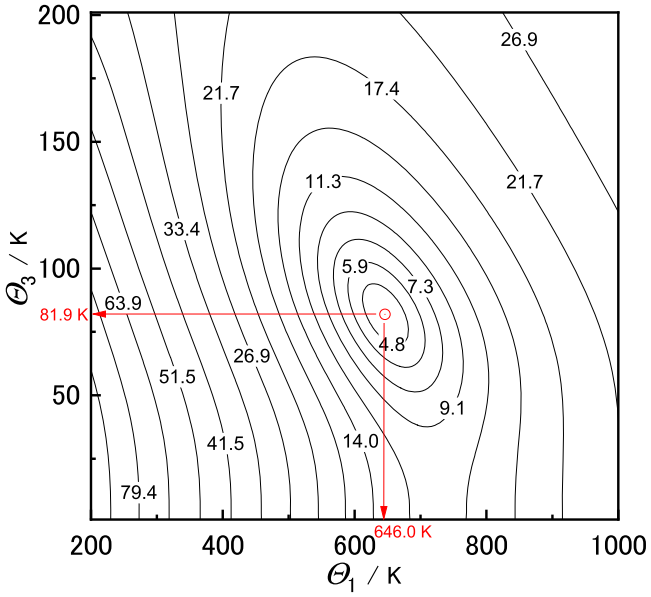

Fig. 4. Contour map of the RMSEs calculated from Eq. (10) based on the fitting of the experimental skeletal heat capacity to a Tarasov function with the characteristic parameters Θ_1 and Θ_3.

following equation is obtained by the least-squares method:

$$C_P^{\text{liquid}} = \left(0.2909\ \text{J K}^{-2}\ \text{mol}^{-1}\right)\cdot T + 101.9\ \text{J K}^{-1}\ \text{mol}^{-1} \quad (15)$$

Using Eq. (15), the heat capacity of PVP in the liquid state at 430−600 K was calculated, and the results are shown in the C_P^{cal} column of Table 2. As shown in Fig. 2, PVP decomposes above 580 K at a heating rate of 10 K min^{-1}. However, according to the reaction kinetics of thermal degradation, there is a heating rate dependence of degradation temperature. For example, the melting point of polyacrylonitrile (PAN) is not observed due to thermal degradation, but when the temperature is increased rapidly using fast scanning calorimetry, the degradation

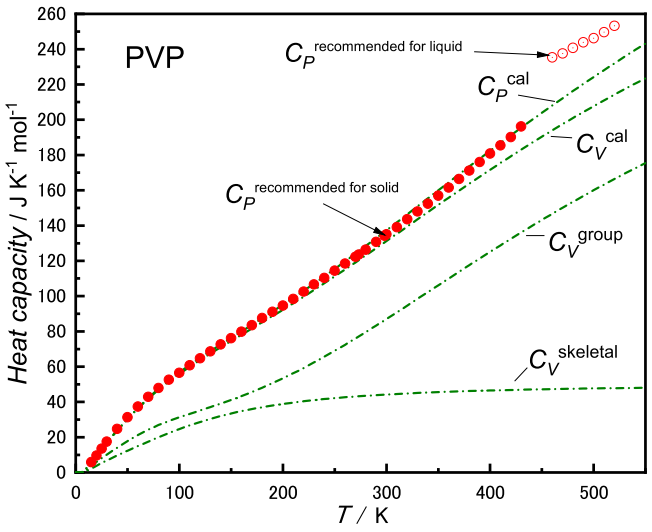

Fig. 5. Heat capacities of PVP. Closed and open circles represent the $C_P^{\text{recommended}}$ for solid and liquid, respectively. The single-pointed curves are calculated from the approximate group vibrational spectrum and skeletal vibrations.

temperature shifts to the high temperature side and the melting point of PAN is observed [32]. Therefore, it is significant to show the calculated heat capacity up to 600 K in PVP.

Table 7
Recommended thermodynamic data for liquid PVP[a].

T / K	$H_T^{\text{l}} - H_0^{\text{c}}$ / J mol^{-1}	$S_T^{\text{l}} - S_0$ / J K^{-1} mol^{-1}	$-(G_T^{\text{l}} - H_0^{\text{c}} + T\,S_0)$ / J mol^{-1}
440.0 (T_g)	45,321	210.22	47,178
450.0	47,726	215.62	49,304
460.0	50,003	220.63	51,488
470.0	52,438	225.88	53,726
480.0	54,748	230.72	55,999
490.0	57,269	235.93	58,338
500.0	59,663	240.76	60,719
510.0	62,214	245.84	63,162
520.0	64,641	250.51	65,626
530.0	67,278	255.56	68,170
540.0	69,789	260.24	70,741
550.0	72,456	265.16	73,384
560.0	74,999	269.70	76,032
570.0	77,753	274.61	78,775
580.0	80,380	279.16	81,530
590.0	83,164	283.95	84,368

[a] H_T^{l}, S_T^{l} and G_T^{l} are the enthalpy, entropy and Gibbs energy at T for anhydrous liquid PVP and H_0^{c} is the enthalpy of a hypothetical crystal for PVP at $T = 0$. These data were calculated from C_P^{cal} obtained by linear approximation to $C_P^{\text{recommended}}$ in Table 2. $C_P^{\text{recommended}}$ was determined from the heat capacities measured by DSC at an atmospheric pressure of 100.25 ± 0.07 kPa.

Table 6
Recommended thermodynamic data for solid PVP[a].

T / K	$H_T^{\text{s}} - H_0^{\text{c}}$ / J mol^{-1}	S_T^{s} / J K^{-1} mol^{-1}	$-(G_T^{\text{s}} - H_0^{\text{c}})$ / J mol^{-1}	T / K	$H_T^{\text{s}} - H_0^{\text{c}}$ / J mol^{-1}	S_T^{s} / J K^{-1} mol^{-1}	$-(G_T^{\text{s}} - H_0^{\text{c}})$ / J mol^{-1}
15.0	24	2.14	8	298.15	21,837	148.22	22,353
20.0	64	4.36	24	300.0	22,091	149.07	22,632
25.0	122	6.94	52	310.0	23,487	153.66	24,147
30.0	199	9.71	93	320.0	24,928	158.23	25,705
40.0	404	15.58	220	330.0	26,414	162.79	27,306
50.0	675	21.62	406	340.0	27,946	167.37	28,961
60.0	1,011	27.72	652	350.0	29,523	171.95	30,659
70.0	1,405	33.79	959	360.0	31,145	176.51	32,400
80.0	1,855	39.79	1,328	370.0	32,813	181.07	34,183
90.0	2,355	45.68	1,756	380.0	34,525	185.65	36,021
100.0	2,901	51.42	2,241	390.0	36,283	190.22	37,902
110.0	3,490	57.02	2,783	400.0	38,085	194.78	39,826
120.0	4,120	62.51	3,382	410.0	39,930	199.32	41,791
130.0	4,789	67.87	4,034	420.0	41,820	203.89	43,812
140.0	5,496	73.11	4,739	430.0	43,753	208.44	45,875
150.0	6,240	78.23	5,494	440.0	45,729	212.98	47,981
160.0	7,022	83.28	6,303	450.0	47,747	217.50	50,128
170.0	7,840	88.25	7,162	460.0	49,807	222.04	52,331
180.0	8,696	93.13	8,068	470.0	51,908	226.56	54,576
190.0	9,590	97.95	9,021	480.0	54,051	231.07	56,862
200.0	10,521	102.74	10,027	490.0	56,233	235.56	59,190
210.0	11,492	107.48	11,079	500.0	58,456	240.06	61,573
220.0	12,502	112.18	12,177	510.0	60,718	244.54	63,998
230.0	13,552	116.83	13,319	520.0	63,019	249.01	66,464
240.0	14,643	121.49	14,513	530.0	65,357	253.45	68,971
250.0	15,777	126.12	15,752	540.0	67,734	257.90	71,533
260.0	16,952	130.72	17,036	550.0	70,148	262.34	74,137
270.0	18,171	135.31	18,363	560.0	72,599	266.75	76,780
273.2	18,564	136.77	18,794	570.0	75,086	271.14	79,463
280.0	19,433	139.92	19,743	580.0	77,608	275.54	82,203
290.0	20,740	144.50	21,164	590.0	80,166	279.91	84,982

[a] H_T^{s}, S_T^{s} and G_T^{s} are the enthalpy, entropy and Gibbs energy at T for anhydrous solid PVP, H_0^{c} is the enthalpy of a hypothetical crystal for PVP at $T = 0$ and S_0 is the residual entropy at $T = 0$. These data were calculated from C_P^{cal} in Tables 1 and 14. C_P^{cal} was obtained by the following procedure: first, C_V^{exp} was calculated by substituting $C_P^{\text{recommended}}$ in Table 1 for C_P^{exp} in Eq. (1), which was then substituted into Eq. (6) to obtain $C_P^{\text{skeletal-exp}}$; then the characteristic parameters Θ_1 and Θ_3, which minimize the RMSE in Eq. (10), were determined; and using those characteristic parameters, C_P^{cal} was calculated from Eqs. (9), (11) and (12). The $C_P^{\text{recommended}}$ values in Table 1 were determined from the heat capacities measured by DSC at an atmospheric pressure of 100.25 ± 0.07 kPa and by adiabatic calorimetry at 298.95 K and an atmospheric pressure of 99.44 ± 0.09 kPa in a calorimeter that was filled with helium and then sealed.

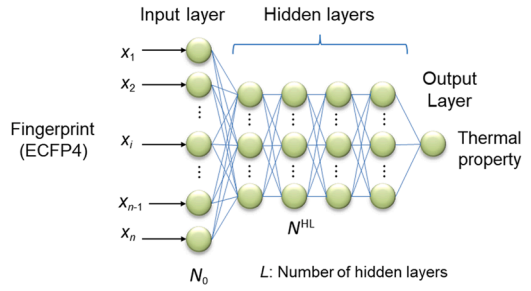

Fig. 6. Hidden-layer structure of the artificial neural network in machine learning for the thermal properties of polymers based on the ATHAS data bank.

Table 8
Comparison of the experimental values in this work and the predicted values of PVP obtained from quantitative structure-property relationship based on deep learning.

Property[a]	Artificial neural network[b]			Experimental values	Relative error[c] /%
	Number of Nodes N^{HL}	Number of Layers L	Predicted values		
T_g / K	50	7	228	440	-48
ΔC_P^0 / J K^{-1} mol^{-1}	50	7	25.6	29.3	-13
T_m^0 / K	50	7	453	(660)	-
Θ_1 / K	250	3	523	646.0	-19
Θ_3 / K	100	5	69.2	81.9	-16

[a] T_g: glass transition temperature for fully amorphous PVP; ΔC_P^0: change in heat capacity for fully amorphous PVP at T_g; T_m^0: equilibrium melting temperature; Θ_1 and Θ_3: characteristic parameters in Tarasov equation shown in Eq. (9).
[b] See Fig. 6 for N^{HL} and L.
[c] Relative error between predicted and experimental vaules.

Table 9
Comparison of the predicted heat capacities by ML and the reccomended heat capacities ($C_P^{recommended}$) of PVP as a function of temperature.

T / K	$C_P^{recommended}$ [a] / J mol^{-1} K^{-1}	Method A[b] Predicted C_P / J K^{-1} mol^{-1}	Relative Error /%	Method B[c] Predicted C_P / J K^{-1} mol^{-1}	Relative Error /%
50	31.3	20.3	-35	33.6	7
100	56.5	39.1	-31	61.9	10
150	76.2	50.1	-34	81.3	7
200	94.6	62.5	-34	99.7	5
250	114.4	79.1	-31	119.9	5
300	135.0	93.0	-31	142.2	5
350	156.9	106.1	-32	165.5	5
400	180.8	120.9	-33	189.0	4

[a] The values are taken from Table 1.
[b] The C_P was predictedby by ML based on the heat capacity registered on ATHAS data bank using the optimal ANN(artificial neural network)-equivalent structures at each temperature.
[c] The C_P was calculated using $\Theta_1 = 523$ K, $\Theta_3 = 69.2$ K and $T_m^0 = 453$ K that were predicted by ML using the optimal ANN-equivalent structures.

5. Discussion

5.1. Heat capacity of solid PVP

The $C_P^{recommended}$ for solid PVP, as shown in Table 1, was applied to Eqs. (1)–(12) to analyze the heat capacity based on the group and skeletal vibrations. First, the experimental constant-volume heat capacity (C_V^{exp}) was calculated by substituting $C_P^{recommended}$ into Eq. (1). The approximate universal constant (3.9×10^{-3} K mol J^{-1}) was used for A'_0 in Eq. (1). The equation also requires a value for T_m^0, but because PVP is an amorphous polymer, no melting point is observed. In general, it is known that the ratio of the glass transition temperature to the melting point is two thirds for all polymers, not just symmetrical or asymmetrical repeating structural units [33]. Using this relationship, the melting point can be calculated as 660 K hypothetically (i.e., assuming the existence of crystals) from the T_g of 440 K. Therefore, this value is used as T_m^0 in the empirical Eq. (1).

When calculating C_V^{group} based on Eq. (2), all the group vibrations of PVP are needed. The vibrational frequencies of the main chain of PVP and its number densities were determined from the similar structure $(CH_2\text{-}CHR\text{-})_n$ of polyethylene and polypropylene, as shown in Table 3 [9,18,34]. In this table, the frequencies are converted to K units by multiplying the value in cm^{-1} by 1.4388.

However, the group vibrations of the 2-pyrrolidone ring have not yet been registered in the ATHAS data bank and there have been no reports on all of its group vibrations. Hence, for calculating the group vibrations of the 2-pyrrolidone ring in PVP, *ab initio* calculations based on the density functional theory were carried out using the GAMESS (US) software package [35] based on the B3LYP/6-311++G** level of theory. The hydrogen-terminated PVP dimer, $H(CH_2\text{-}CHR)_2H$, where R represents 2-pyrrolidone (C_4H_7NO), was employed for the calculation model of PVP so that the vibrational calculation could be performed at a reasonable computational cost.

The molecular geometry of the hydrogen-terminated PVP dimer was first optimized and then it was confirmed that the optimized structure had no imaginary frequencies. After geometry optimization, the vibration spectra of the dimer were calculated and assignments of the vibrators were made. By using the dimer, the number of 2-pyrrolidone-ring-derived vibrators was doubled and two close vibrational frequencies were obtained for each oscillator. When the two vibrational frequencies were less than 10 cm^{-1} apart, they were averaged and approximated by the Einstein function in Eq. (3). However, when the two frequencies were more than 10 cm^{-1} apart, they were approximated by the box distribution in Eq. (5). Finally, the 34 group vibrations of the 2-pyrrolidone ring were determined as summarized in Table 4.

The group and skeletal vibrations are summarized in Table 5. There are 11 vibrators in the main chain of PVP and 34 in the pyrrolidone ring. Since the number of atoms in the repeating structural unit of PVP is 17, there are 51 (= 3 × 17) vibrators, and by subtracting the number of group vibrations, 45 (= 34+11), the number of skeletal vibrations (N_s) can be determined to be six. Substituting the value of N_s into either Eq. (7) or (9), $C_V^{skeletal\_cal}$ can be calculated.

C_V^{group} was calculated using the group frequencies shown in Tables 3, 4 and Eq. (2), and then was substituted into Eq. (6) to calculate $C_V^{skeletal\_exp}$. In contrast, $C_V^{skeletal\_cal}$ was calculated from Eq. (9) using the characteristic parameters Θ_1 and Θ_3. A mesh optimization was carried out to find the point where the RMSE in Eq. (10) is minimum, and to obtain the values of the characteristic parameters. For efficient calculation of Θ_1 and Θ_3, the following three steps were performed.

(i) Wide scan: $C_V^{skeletal\_cal}$ is calculated as a function of temperature on a 41 × 19 mesh with Θ_1 from 200 to 1000 K in 20 K increments and Θ_3 from 10 to 200 K in 10 K increments, and the RMSE is calculated from Eq. (10). Then, one finds Θ_1 and Θ_3 when the RMSE is minimum.
(ii) Middle scan: Using a 21 × 21 mesh with a range of ± 10 K in 1 K increments for each of Θ_1 and Θ_3 obtained in (i) above, one finds the improved Θ_1 and Θ_3 when the RMSE is minimum.
(iii) Narrow scan: Using a 41 × 41 mesh with a range of ± 2 K in 0.1 K increments for each of Θ_1 and Θ_3 obtained in (ii) above, one finds Θ_1 and Θ_3 with higher precision when the RMSE is minimum.

Fig. 4 shows the results of RMSE-contour plots obtained by wide scan. Based on these results, mesh optimization by middle scan and narrow scan was performed sequentially and $\Theta_1 = 646.0$ K and $\Theta_3 =$

Table 10
Sample specifications.

ChemicalName	Source	Initial purity wt%	mol%	PurificationMethod	FinalPurity	AnalysisMethod
poly(*N*-vinylpyrrolidone) (CAS: 9003-39-8)	Sigma–Aldrich (Lot # STBJ3834, 234257)	93.2[e]	-	Heat treatment for dehydration	-[f]	TG[a], TG-MS[b] and GPC-MALS[c]
a-Al_2O_3 (Sapphire disk)	NETZSCH Gerätebau (Series No. 2466)	99.99	-	none	-	-
Indium	LGC Standards LGC2601 (No.2126)	-	99.99998	none	-	Adiabatic calorimetry
Tin	LGC Standards LGC2609 (No.5329)	-	99.9995	none	-	Adiabatic calorimetry
Distilled water	FUJIFILM Wako Pure Chemical 042-16973	> 99.9995[g]	-	none	-	Evaporation
Octane	FUJIFILM Wako Pure Chemical 153-00065 (No.ESL2978)	> 98	-	none	-	GC[d]

[a] Thermogravimetry.
[b] Thermogravimetry-Mass spectroscopy.
[c] Gel permeation chromatograph-multi angle light scattering.
[d] Gas chromatography.
[e] The value was measured by TG, as shown in Fig. 2. Using TG-MS, the impurity was confirmed to be water.
[f] For the PVP sample after being heated at 373 K for 30 min and then further heated at 473 K for 10 min, no impurity peaks were observed in the GPC-MALS measurement. Furthermore, heat treatment was performed at 520 K in the DSC cell prior to measurement; the purity of the samples could not be confirmed because they immediately absorbed moisture upon removal from the DSC cell. However, considering that the weight loss between 520–550 K was 0.16 wt% (shown in Fig. 2) and that the weight loss includes the pyrolysis of PVP, the residual water content would be estimated as below 0.16 wt%.
[g] Non-volatile matter is less than 5 ppm.

81.9 K were determined from the minimum value of the RMSE. Note that the characteristic parameters were obtained by the mesh optimization using Eq. (7) but no drastic improvement of the RMSE in Eq. (10) was observed, therefore Eq. (9) (i.e., $\Theta_2 = \Theta_3$) was used in this study.

$C_V^{\text{skeletal\_cal}}$ was calculated from Eq. (9) using Θ_1 and Θ_3 obtained by the three-step mesh optimization, and C_V^{group} was added to it to calculate C_V^{cal} from Eq. (11). Then, C_P^{cal} was calculated from Eq. (12). The results are shown in Fig. 5 and Table 1. C_P^{cal} is in good agreement with $C_P^{\text{recommended}}$, indicating that C_P^{cal} is close to the experimental data. Based on C_P^{cal}, it is possible to estimate the heat capacity at high temperatures that cannot be measured by pyrolysis, and also to determine the baseline of DSC.

5.2. Heat capacity of liquid PVP and change of heat capacity at the glass transition

As the temperature is high enough in the liquid state, the intermolecular skeletal vibrations are fully excited so that additivity holds for both the intramolecular skeletal vibrations and the group vibrations [10]. A linear relationship for the temperature dependence of heat capacity in liquid polymers and additivity due to structural groups has been reported for aliphatic nylons [30], aliphatic polyesters [36] and aliphatic polyoxides [31]. Furthermore, for poly(*N*-isopropylacrylamide), the heat capacities calculated from additivity due to suitable structural groups were reported to be in good agreement with the measured values [37]. However, the contribution of the pyrrolidone ring to the heat capacity of the liquid state has not been reported, therefore the heat capacity of the liquid PVP could not be estimated. Thus, the contribution of the pyrrolidone ring to the heat capacity of liquid PVP was determined using the experimental values obtained in this study. The following equation is expected to hold for the heat capacity of liquid PVP:

$$C_P^{\text{liquid}}(\text{cal}) = N_{\text{CHCH}_2}\left[(0.1314\ \text{J K}^{-2}\ \text{mol}^{-1})\cdot T + 10.4\ \text{J K}^{-1}\ \text{mol}^{-1}\right] + N_{\text{pyrrolidone}}\ (\text{A}\ T + B) \quad (16)$$

where N_{CHCH_2} and $N_{\text{pyrrolidone}}$ are the number of the respective groups in the repeating unit of PVP, and A and B are unknown constants. By combining Eq. (15), $N_{\text{CHCH}_2} = 1$ and $N_{\text{pyrrolidone}} = 1$, we obtain $A = 0.1595$ and $B = 91.6$. Therefore, the heat capacity contribution from the pyrrolidone ring in the polymer is determined to be $N_{\text{pyrrolidone}}$ (0.1595 T + 91.6) in J K^{-1} mol^{-1}.

The T_g of PVP is determined to be 440 K based on the intersection of the midline obtained from the baselines before and after the glass transition. The change in heat capacity at the glass transition for amorphous PVP (ΔC_P^0) could be determined from the extrapolated solid and liquid heat capacities at T_g and hence ΔC_P^0 at T_g for PVP is determined to be 29.3 J K^{-1} mol^{-1}. In reference [6], the T_g and ΔC_P° for PVP were reported to be 442 K and 30.4 J K^{-1} mol^{-1}, respectively, which are in good agreement with the results in this study. In addition, in reference [38], the onset temperature of the glass transition of PVP with a molecular weight of 50,000 g mol^{-1} at a heating rate of 10 K min^{-1} was reported to be 434 K, which is in close agreement with the onset temperature (433 K) obtained from Fig. 3.

The contribution of the small mobile beads in the repeating unit (such as CH_2-, O− or $CHCH_3-$) is reported to be 11.5 ± 1.7 J K^{-1} mol^{-1}, whereas that of the large beads (such as C_6H_4-) is double or triple that of a small bead [7,10]. For example, the repeating unit of polystyrene has both one small bead and one large bead, and the ΔC_P^0 is 30.8 J mol^{-1} K^{-1} [7,10]. Similarly, that of PVP also has both one small bead and one large bead, thus the ΔC_P^0 value would be reasonable.

5.3. Thermodynamic functions for PVP

With the heat capacities known over the full temperature range, one can also derive enthalpies, entropies and Gibbs energies using the following equations:

$$H = H_0 + \int_0^T C_P\, dT \quad (17)$$

$$S = S_0 + \int_0^T (C_P / T)\, dT \quad (18)$$

$$G = H - TS \quad (19)$$

Considering a hypothetical crystal H_0 (denoted H_0^C), thermodynamic functions for solid PVP can be obtained from Eqs. (17)–(19), as shown in Table 6. However, thermodynamic data for liquid PVP above T_g were calculated by assuming that the heat capacity of the liquid is the same as that of the solid below T_g. The calculation results are shown in Table 7.

Table 11
Experimental values of heat capacities measured by adiabatic calorimetry for moisture-absorbed PVP[a].

T[b] / K	C_P[c] / J K^{-1} g^{-1}	T / K	C_P / J K^{-1} g^{-1}	T / K	C_P / J K^{-1} g^{-1}	T / K	C_P / J K^{-1} g^{-1}	T / K	C_P / J K^{-1} g^{-1}	T / K	C_P / J K^{-1} g^{-1}
(Series 1)		62.20	0.3694	137.02	0.7098	251.84	1.2212	283.12	1.3941	219.05	1.0545
10.65	0.02295	63.67	0.3788	139.01	0.7180	254.83	1.2363	286.10	1.4108	222.04	1.0701
11.42	0.02703	65.13	0.3868	141.00	0.7267	257.81	1.2528	289.08	1.4291	225.02	1.0817
12.20	0.03155	66.60	0.3938	142.99	0.7334	260.79	1.2694	292.06	1.4465	228.01	1.0963
12.99	0.03634	68.07	0.4021	144.98	0.7404	263.77	1.2844	295.04	1.4638	231.00	1.1104
13.80	0.04093	69.54	0.4101	146.97	0.7503	266.75	1.3020	298.03	1.4814	233.99	1.1265
14.63	0.04616	71.01	0.4178	148.95	0.7573	269.74	1.3204	301.01	1.4985	236.97	1.1412
15.48	0.05198	72.49	0.4256	150.94	0.7664	272.72	1.3368	304.00	1.5173	239.96	1.1575
16.42	0.05791	73.96	0.4324	153.43	0.7756	275.71	1.3518	306.98	1.5335	242.95	1.1710
17.41	0.06478	75.44	0.4405	156.41	0.7881	278.69	1.3685	309.96	1.5520	245.93	1.1862
18.48	0.07250	76.92	0.4471	159.39	0.7984	281.66	1.3865	312.95	1.5699	248.91	1.2038
19.61	0.08107	78.40	0.4554	162.36	0.8112	284.64	1.4008	315.93	1.5891	251.89	1.2205
20.92	0.08991	79.87	0.4623	165.33	0.8240	287.61	1.4200	318.92	1.6052	254.87	1.2369
22.12	0.09931	81.59	0.4703	168.31	0.8323	290.59	1.4375	321.91	1.6243	257.85	1.2542
23.34	0.1084	83.56	0.4799	171.29	0.8440	293.57	1.4552	324.89	1.6427	260.84	1.2698
24.59	0.1179	85.52	0.4882	174.27	0.8580	296.55	1.4724	327.88	1.6603	263.82	1.2863
25.86	0.1288	87.49	0.4975	177.26	0.8688	299.52	1.4911	330.86	1.6781	266.81	1.3036
27.14	0.1382	89.46	0.5060	180.24	0.8808	302.51	1.5086	333.84	1.6983	269.79	1.3201
28.43	0.1475	91.43	0.5151	183.22	0.8921	305.49	1.5326	(Series 3)		272.77	1.3365
30.88	0.1636	93.40	0.5234	186.20	0.9065	308.45	1.5548	153.43	0.7764	275.75	1.3530
32.22	0.1745	95.37	0.5324	189.18	0.9182	311.42	1.5828	156.41	0.7871	278.73	1.3688
33.58	0.1845	97.34	0.5407	192.16	0.9324	314.37	1.6084	159.39	0.7992	281.71	1.3856
34.96	0.1945	99.32	0.5499	195.15	0.9465	317.35	1.6324	162.37	0.8107	284.68	1.4024
36.33	0.2049	101.29	0.5576	198.13	0.9598	320.34	1.6538	165.34	0.8228	287.66	1.4204
37.72	0.2148	103.26	0.5662	201.12	0.9728	323.36	1.6755	168.33	0.8325	290.63	1.4384
39.12	0.2236	105.24	0.5738	204.10	0.9857	326.39	1.6907	171.31	0.8445	293.61	1.4557
40.53	0.2335	107.22	0.5823	207.09	0.9997	329.43	1.7063	174.29	0.8573	296.59	1.4714
41.95	0.2424	109.20	0.5920	210.07	1.0147	332.47	1.7254	177.27	0.8684	299.57	1.4905
43.36	0.2518	111.19	0.5990	213.05	1.0267	335.52	1.7464	180.26	0.8804	302.55	1.5096
44.78	0.2605	113.17	0.6083	216.03	1.0403	(Series 2)		183.24	0.8925	305.53	1.5267
46.20	0.2702	115.16	0.6168	219.02	1.0553	250.34	1.2104	186.22	0.9062	308.51	1.5437
47.62	0.2795	117.14	0.6253	222.00	1.0693	253.32	1.2293	189.21	0.9194	311.50	1.5606
49.05	0.2889	119.13	0.6328	224.99	1.0832	256.30	1.2454	192.19	0.9322	314.49	1.5793
50.48	0.2987	121.11	0.6419	227.97	1.0959	259.28	1.2621	195.18	0.9466	317.47	1.5969
51.99	0.3092	123.10	0.6514	230.95	1.1112	262.26	1.2791	198.16	0.9606	320.45	1.6160
53.43	0.3183	125.09	0.6594	233.94	1.1268	265.25	1.2959	201.15	0.9735	323.43	1.6356
54.89	0.3278	127.08	0.6684	236.92	1.1419	268.23	1.3114	204.13	0.9867	326.42	1.6553
56.35	0.3367	129.07	0.6758	239.90	1.1562	271.20	1.3291	207.11	1.0010	329.40	1.6762
57.81	0.3452	131.06	0.6837	242.89	1.1699	274.18	1.3450	210.09	1.0140	332.39	1.6967
59.27	0.3541	133.05	0.6936	245.87	1.1877	277.16	1.3601	213.08	1.0268	335.37	1.7175
60.73	0.3614	135.03	0.7020	248.86	1.2049	280.14	1.3778	216.07	1.0396		

[a] The PVP sample was in the glassy state.
[b] The resolution of the thermometry was ± 0.3 mK at 15 K and ± 0.06 mK at 80 K [20], and the inaccuracy of the calibrated temperature was ± 0.36% at 4.2 K, ± 0.030% at 100 K and ± 0.012% at 300 K.
[c] C_P represents the experimental data measured by adiabatic calorimetry for moisture-absorbed PVP at 297.65 K and an atmospheric pressure of 100.94±0.05 kPa in a calorimeter that was filled with helium and then sealed. The water content was 8.82 wt%. The inaccuracy of the heat capacity measurement was 1% for T < 30 K, 0.5% for 30 K < T < 60 K and 0.3% for T > 60 K.

Here, H_T^s, S_T^s and G_T^s represent the enthalpy, entropy and Gibbs energy at T for solid PVP; H_T^l, S_T^l and G_T^l represent the enthalpy, entropy and Gibbs energy at T for liquid PVP; and H_0^c and S_0 represent the enthalpy of a hypothetical crystal for PVP and the residual entropy at $T = 0$, respectively. Lebedev et al. reported thermodynamic functions for PVP of: $H_T^s - H_0 = 25.17$ kJ mol^{-1}, $S_T^s - S_0 = 195.7$ J K^{-1} mol^{-1} and $G_T^s - H_0 + T S_0 = -24.64$ kJ mol^{-1} at 298.15 K [25]. The aforementioned effect of residual moisture probably resulted in slightly different results from the values shown in Table 6.

5.4. Comparison of experimental and predicted values by deep leaning using the ATHAS data bank

It has already been reported that the thermal properties of polymers can be predicted by deep learning based on the ATHAS data bank [39]. Using the artificial neural network (ANN)- structure as shown in Fig. 6, the thermal properties of PVP can be predicted.

The equivalent structure for the hidden layer, where the number of nodes in all hidden layers is equal, was adopted for machine learning using artificial neural networks. The predicted thermal properties for PVP are shown in Table 8, which also shows the structure of the optimized ANN hidden layer obtained according to the method described in Ref. [39]. For T_g, there is a large discrepancy between the predicted and experimental values with a relative error of 48%. The reason may be that the prediction using machine learning is extrapolated from the quantitative structure–property relationship (QSPR) because polymers with the pyrrolidone ring in the repeating structural unit are not registered in the ATHAS data bank, and the actual T_g of PVP increases due to the formation of a hydrogen bonding network. However, for ΔC_P^0, Θ_1, and Θ_3, despite extrapolation of the QSPR, the predictions were made within a relative error of 20%.

Table 9 shows the comparison between the predicted values by deep learning and the experimental heat capacity of PVP as a function of temperature. Two methods were used to obtain the predicted values. One is to perform deep learning on the heat capacity at each temperature registered in the ATHAS data bank and then predict the heat capacity of PVP at each temperature using the learned model. The other method is to predict Θ_1, Θ_3 and T_m^0 of PVP by deep learning as shown in Table 8, and then substitute those values into Eqs. (9), (11), and (12) to calculate the heat capacity of PVP as a function of temperature. As shown in

Table 12
Heat capacities determined using adiabatic calorimetry for dried PVP[a].

T[b] K	C_P[c] J K^{-1} g^{-1}	T K	C_P J K^{-1} g^{-1}	T K	C_P J K^{-1} g^{-1}	T K	C_P J K^{-1} g^{-1}	T K	C_P J K^{-1} g^{-1}	T K	C_P J K^{-1} g^{-1}
(Series 4)		55.14	0.3139	119.37	0.5915	214.30	0.9278	215.82	0.9348	326.25	1.3869
9.13	0.01894	56.60	0.3235	121.35	0.6007	217.29	0.9412	218.80	0.9478	329.24	1.4004
10.12	0.02327	58.05	0.3307	123.34	0.6080	220.27	0.9531	221.79	0.9567	332.23	1.4148
11.09	0.02898	59.51	0.3378	125.33	0.6147	223.26	0.9608	224.78	0.9691	335.21	1.4255
12.04	0.03394	60.96	0.3475	127.31	0.6228	226.25	0.9723	227.76	0.9810	(Series 6)	
12.98	0.03953	62.42	0.3543	129.30	0.6292	229.24	0.9875	230.76	0.9941	259.15	1.1066
13.92	0.04554	63.88	0.3617	131.30	0.6354	232.23	0.9987	233.75	1.0031	262.14	1.1183
14.86	0.05126	65.35	0.3700	133.29	0.6444	235.22	1.0105	236.74	1.0173	265.13	1.1286
15.88	0.05768	66.82	0.3766	135.27	0.6511	238.21	1.0224	239.73	1.0274	268.11	1.1395
16.94	0.06466	68.28	0.3836	137.26	0.6576	241.20	1.0322	242.73	1.0379	271.09	1.1527
18.08	0.07252	69.75	0.3902	139.25	0.6655	244.19	1.0462	245.71	1.0513	274.08	1.1634
19.27	0.08081	71.22	0.3981	141.23	0.6728	247.18	1.0590	248.70	1.0641	277.06	1.1756
20.51	0.08970	72.69	0.4048	143.23	0.6788	250.17	1.0703	251.68	1.0756	280.05	1.1880
21.86	0.10021	74.17	0.4109	145.22	0.6862	253.15	1.0816	254.67	1.0881	283.04	1.2020
23.15	0.1086	75.64	0.4185	147.21	0.6919	256.15	1.0947	257.65	1.0989	286.02	1.2145
24.44	0.1179	77.12	0.4242	149.19	0.6996	(Series 5)		260.63	1.1125	289.01	1.2276
25.76	0.1277	78.60	0.4320	151.68	0.7064	153.20	0.7127	263.62	1.1241	292.00	1.2405
27.09	0.1370	80.08	0.4384	154.66	0.7169	156.17	0.7230	266.60	1.1356	294.99	1.2535
28.44	0.1455	81.80	0.4452	157.63	0.7278	159.14	0.7334	269.59	1.1460	297.97	1.2659
29.75	0.1560	83.77	0.4550	160.60	0.7379	162.12	0.7424	272.57	1.1580	300.95	1.2780
31.10	0.1643	85.74	0.4624	163.58	0.7481	165.10	0.7545	275.55	1.1706	303.94	1.2899
32.47	0.1744	87.71	0.4709	166.56	0.7581	168.08	0.7635	278.53	1.1834	306.92	1.3019
33.83	0.1836	89.67	0.4792	169.53	0.7684	171.06	0.7749	281.51	1.1946	309.91	1.3142
35.21	0.1930	91.65	0.4884	172.51	0.7781	174.04	0.7845	284.49	1.2089	312.89	1.3279
36.58	0.2013	93.63	0.4941	175.50	0.7907	177.02	0.7961	287.47	1.2224	315.87	1.3429
37.97	0.2114	95.61	0.5020	178.48	0.7998	179.99	0.8073	290.46	1.2357	318.85	1.3543
39.37	0.2201	97.59	0.5089	181.46	0.8111	182.98	0.8171	293.44	1.2453	321.84	1.3681
40.78	0.2290	99.56	0.5162	184.44	0.8212	185.96	0.8263	296.43	1.2575	324.82	1.3805
42.20	0.2376	101.54	0.5247	187.42	0.8320	188.94	0.8387	299.41	1.2735	327.80	1.3938
43.60	0.2460	103.52	0.5321	190.41	0.8427	191.93	0.8486	302.39	1.2834	330.78	1.4070
45.02	0.2558	105.50	0.5396	193.40	0.8541	194.91	0.8597	305.38	1.2957	333.76	1.4198
46.45	0.2631	107.48	0.5471	196.38	0.8641	197.89	0.8699	308.36	1.3088	336.74	1.4313
47.88	0.2715	109.46	0.5556	199.37	0.8747	200.88	0.8796	311.34	1.3224		
49.31	0.2800	111.44	0.5615	202.35	0.8861	203.87	0.8921	314.32	1.3358		
50.79	0.2900	113.42	0.5708	205.34	0.8948	206.85	0.9031	317.30	1.3484		
52.24	0.2967	115.41	0.5778	208.33	0.9067	209.84	0.9120	320.29	1.3614		
53.70	0.3051	117.39	0.5855	211.32	0.9179	212.83	0.9244	323.27	1.3743		

[a] Before heat capacity measurements, the PVP sample was heated at 473 K for 10 min after being heated at 373 K for 30 min. The residual water content was 1.89 wt %. The solid PVP sample was in the glassy state.

[b] The resolution of the thermometry was ± 0.3 mK at 15 K and ± 0.06 mK at 80 K [20], and the inaccuracy of the calibrated temperature was ± 0.36% at 4.2 K, ± 0.03% at 100 K and ± 0.012% at 300 K.

[c] C_P represents the heat capacity data determined by adiabatic calorimetry for anhydrous PVP at 298.95 K and an atmospheric pressure of 99.44 ± 0.09 kPa. in a calorimeter that was filled with helium and then sealed. The inaccuracy of the heat capacity measurement was 1% for T < 30 K, 0.5% for 30 K < T < 60 K and 0.3% for T > 60 K.

Table 9, the relative errors between the experimental $C_P^{\text{recommended}}$ and predicted values are in the range of −31% to −34% for the former method, while those are in the range of 4% to 10% for the latter method, indicating that the latter is the better method for predicting heat capacity. In other words, for calculation of the temperature dependence of the heat capacity, it is better to predict Θ_1, $\mathbf{\Theta}_3$ and T_m^0 by deep learning and then to apply the ATHAS method described in Section 2 using these values rather than directly calculating the heat capacity using the QSPR between repeating chemical structure and heat capacity at each temperature by deep learning. This finding is consistent with the prediction results for the temperature dependence of the heat capacity of poly(*p*-dioxanone) reported in a previous paper [39].

6. Conclusion

It was possible to derive a data set for heat capacity over a temperature range from 9 K to 520 K for a dried amorphous polyvinylpyrrolidone (PVP). Based on the recommended values, the heat capacity of the sold state was analyzed using an approximate group vibrational spectrum and skeletal vibrations, after the 2-pyrrolidone ring group vibrations have been determined based on the *ab initio* calculations. The characteristic parameters for the Tarasov equation, Θ_1 and Θ_3, were determined to be 646.0 K and 81.9 K, respectively, using a three-step mesh optimization. The glass transition temperature is 440 K for a heating rate of 10 K min^{-1}. The change in heat capacity at the glass transition ΔC_P^0 is 29.3 J K^{-1} mol^{-1}. The values of ΔC_P^0, Θ_1 and Θ_3 agreed with the deep learning predictions based on the ATHAS databank with a relative error within 20%.

CRediT authorship contribution statement

Kazuhiko Ishikiriyama: Conceptualization, Methodology, Data curation, Validation, Formal analysis, Investigation, Software, Resources, Writing – original draft, Visualization, Supervision, Project administration, Writing – review & editing. **Keisuke Kondo:** Methodology, Data curation, Validation, Formal analysis, Investigation, Resources, Supervision, Writing – review & editing. **Yuji Miyazaki:** Methodology, Data curation, Validation, Formal analysis, Investigation, Resources, Supervision, Writing – review & editing. **Yuto Sasada:** Methodology, Data curation, Validation, Formal analysis, Investigation, Resources, Supervision, Writing – review & editing. **Keisuke Sawada:** Methodology, Data curation, Validation, Formal analysis, Investigation, Resources, Supervision, Writing – review & editing. **Ryo Endo:** Methodology, Data curation, Validation, Formal analysis, Investigation, Resources, Supervision, Writing – review & editing. **Naoki Man:** Methodology, Data curation, Validation, Formal analysis, Investigation,

Table 13
Heat capacities of PVP[a] measured by DSC.

T[b] K	C_P^{DSC}[c] J K^{-1} mol^{-1}	U[d] %	T[b] K	C_P^{DSC}[c] J K^{-1} mol^{-1}	U[d] %	T[b] K	C_P^{DSC}[c] J K^{-1} mol^{-1}	U[d] %	T[b] K	C_P^{DSC}[c] J K^{-1} mol^{-1}	U[d] %	T[b] K	C_P^{DSC}[c] J K^{-1} mol^{-1}	U[d] %	T[b] K	C_P^{DSC}[c] J K^{-1} mol^{-1}	U[d] %
203.70	97.28	0.79	256.71	116.97	1.07	309.81	139.17	1.04	362.99	162.99	1.10	416.16	188.27	0.54	469.23	236.21	0.61
204.70	97.82	0.73	257.71	117.28	1.04	310.82	139.67	1.07	364.00	163.48	1.07	417.16	188.86	0.56	470.23	236.80	0.68
205.70	98.21	0.78	258.71	117.74	1.00	311.82	140.02	1.04	365.00	163.84	1.08	418.16	189.19	0.59	471.23	237.27	0.70
206.70	98.60	0.72	259.71	118.14	1.01	312.82	140.55	1.04	366.00	164.34	1.02	419.17	189.77	0.55	472.22	237.28	0.68
207.71	98.11	1.43	260.71	118.55	1.02	313.83	140.93	1.07	367.01	164.92	1.04	420.17	190.21	0.54	473.22	237.68	0.71
208.71	98.49	1.36	261.72	118.94	1.04	314.83	141.29	1.09	368.01	165.39	1.05	421.17	190.74	0.60	474.22	237.90	0.70
209.71	98.91	1.32	262.72	119.36	1.04	315.83	141.81	1.02	369.01	165.92	1.05	422.17	191.28	0.61	475.22	238.57	0.70
210.71	99.31	1.27	263.72	119.77	1.01	316.83	142.24	1.06	370.02	166.38	1.05	423.18	191.78	0.58	476.22	239.10	0.65
211.71	99.67	1.29	264.72	120.17	0.99	317.84	142.66	1.10	371.02	166.78	1.04	424.18	192.52	0.58	477.22	239.16	0.63
212.71	100.07	1.30	265.72	120.63	1.02	318.84	143.14	1.08	372.02	167.27	1.03	425.18	193.01	0.59	478.22	239.59	0.56
213.72	100.41	1.28	266.72	121.01	1.02	319.84	143.56	1.05	373.03	167.78	0.99	426.18	193.53	0.59	479.22	239.94	0.53
214.72	100.74	1.29	267.72	121.41	1.06	320.85	144.07	1.06	374.03	168.29	0.98	427.18	194.14	0.60	480.22	240.23	0.47
215.72	101.16	1.31	268.72	121.82	1.03	321.85	144.43	1.09	375.03	168.84	0.96	428.19	194.77	0.60	481.22	240.69	0.49
216.72	101.54	1.25	269.72	122.23	1.07	322.85	144.91	1.08	376.04	169.39	0.97	429.19	195.51	0.70	482.22	240.95	0.42
217.72	101.88	1.22	270.73	122.63	1.05	323.86	145.32	1.02	377.04	169.78	1.01	430.19	196.34	0.71	483.22	241.42	0.41
218.73	102.28	1.19	271.73	123.08	1.08	324.86	145.75	1.09	378.04	170.19	1.03	431.19	197.24	0.75	484.21	241.80	0.36
219.73	102.66	1.18	272.73	123.48	0.99	325.86	146.24	1.07	379.05	170.73	1.02	432.19	198.11	0.85	485.21	242.06	0.34
220.73	103.02	1.20	273.73	123.89	1.02	326.87	146.64	1.12	380.05	171.17	0.97	433.20	199.01	0.86	486.21	242.52	0.32
221.73	103.35	1.21	274.73	124.35	1.06	327.87	147.05	1.10	381.05	171.67	0.95	434.20	200.06	0.92	487.21	242.76	0.36
222.73	103.75	1.19	275.73	124.74	0.98	328.87	147.59	1.04	382.06	172.20	0.94	435.20	201.14	1.08	488.21	243.20	0.27
223.73	104.13	1.20	276.74	125.17	1.01	329.88	148.05	1.11	383.06	172.71	0.99	436.20	202.93	1.15	489.21	243.57	0.23
224.72	104.52	1.16	277.74	125.52	1.04	330.88	148.40	1.12	384.06	173.14	0.98	437.20	204.46	1.21	490.20	243.59	0.31
225.72	104.90	1.17	278.74	125.95	1.04	331.88	148.85	1.08	385.07	173.62	0.97	438.20	206.39	1.31	491.20	243.57	0.60
226.72	105.25	1.19	279.74	126.33	1.04	332.89	149.34	1.14	386.07	174.14	0.94	439.21	208.57	1.50	492.20	243.70	0.69
227.72	105.58	1.18	280.74	126.78	1.03	333.89	149.84	1.14	387.07	174.56	0.89	440.21	210.79	1.69	493.20	243.92	0.79
228.72	105.96	1.17	281.74	127.21	1.07	334.89	150.22	1.10	388.08	175.01	0.97	441.21	213.32	1.91	494.20	244.08	0.86
229.72	106.42	1.18	282.75	127.65	1.04	335.90	150.65	1.12	389.08	175.58	0.82	442.21	216.12	2.16	495.19	244.49	0.90
230.72	106.76	1.14	283.75	128.06	1.05	336.90	151.04	1.06	390.08	176.08	0.88	443.21	219.46	2.31	496.19	244.72	0.92
231.71	107.19	1.10	284.75	128.50	1.03	337.90	151.48	1.10	391.09	176.58	0.89	444.21	223.00	2.47	497.19	244.91	0.89
232.71	107.58	1.10	285.75	128.83	1.02	338.91	151.98	1.08	392.09	177.07	0.80	445.21	226.56	2.52	498.19	245.28	0.90
233.71	107.95	1.09	286.75	129.25	1.02	339.91	152.34	1.11	393.09	177.51	0.78	446.21	229.85	2.43	499.19	245.55	0.87
234.71	108.30	1.06	287.76	129.77	1.01	340.91	152.85	1.10	394.10	178.05	0.85	447.22	232.43	2.15	500.18	245.99	0.90
235.71	108.73	1.11	288.76	130.22	0.97	341.92	153.32	1.12	395.10	178.56	0.82	448.22	234.49	1.89	501.18	246.27	1.01
236.71	109.08	1.11	289.76	130.54	1.06	342.92	153.79	1.12	396.10	178.94	0.76	449.22	235.76	1.58	502.18	246.81	0.99
237.71	109.47	1.07	290.76	131.00	1.03	343.93	154.28	1.14	397.11	179.41	0.70	450.22	236.55	1.21	503.17	246.99	0.97
238.71	109.83	1.12	291.77	131.43	1.03	344.93	154.73	1.11	398.11	179.93	0.74	451.22	236.50	0.92	504.17	247.36	0.96
239.71	110.21	1.10	292.77	131.79	1.10	345.93	155.14	1.10	399.11	180.38	0.75	452.22	236.05	0.86	505.17	247.64	1.00
240.71	110.62	1.09	293.77	132.29	1.07	346.94	155.57	1.11	400.12	180.89	0.71	453.22	235.31	0.84	506.17	248.25	1.00
241.71	111.00	1.12	294.77	132.74	1.10	347.94	155.98	1.12	401.12	181.33	0.70	454.22	234.95	0.72	507.16	248.34	1.07
242.71	111.39	1.10	295.78	133.20	1.08	348.94	156.50	1.16	402.12	181.81	0.70	455.22	234.62	0.63	508.16	248.76	1.00
243.71	111.81	1.06	296.78	133.60	1.00	349.95	156.92	1.10	403.12	182.26	0.65	456.22	234.48	0.60	509.16	249.08	1.08
244.71	112.23	1.03	297.78	133.96	1.07	350.95	157.37	1.14	404.13	182.66	0.63	457.22	234.29	0.66	510.15	249.53	1.08
245.71	112.63	1.06	298.78	134.34	1.07	351.95	157.80	1.13	405.13	183.25	0.65	458.22	234.33	0.64	511.15	249.93	1.04
246.71	112.97	1.06	299.79	134.82	1.09	352.96	158.27	1.13	406.13	183.72	0.62	459.22	234.39	0.76	512.15	250.37	1.09
247.71	113.34	1.04	300.79	135.27	1.08	353.96	158.78	1.12	407.14	184.10	0.62	460.23	234.52	0.82	513.14	250.65	1.09
248.71	113.77	1.02	301.79	135.75	1.04	354.96	159.23	1.16	408.14	184.62	0.62	461.23	234.68	0.82	514.14	251.12	1.14
249.71	114.10	1.07	302.79	136.10	1.04	355.97	159.80	1.06	409.14	185.10	0.64	462.23	234.77	0.81	515.13	251.33	1.13
250.71	114.55	1.08	303.80	136.59	1.05	356.97	160.34	1.04	410.14	185.54	0.56	463.23	235.04	0.80	516.13	251.87	1.09
251.71	114.93	1.02	304.80	136.98	1.08	357.97	160.80	1.04	411.15	185.99	0.59	464.23	235.49	0.80	517.13	252.26	1.14
252.71	115.34	1.07	305.80	137.37	1.03	358.98	161.16	1.11	412.15	186.47	0.60	465.23	235.74	0.87	518.12	252.71	1.20
253.71	115.74	1.06	306.80	137.82	1.01	359.98	161.54	1.05	413.15	186.89	0.61	466.23	235.97	0.82	519.12	252.97	1.18
254.71	116.16	1.07	307.81	138.28	1.03	360.99	162.10	1.05	414.15	187.37	0.57	467.23	236.37	0.78			
255.71	116.59	1.07	308.81	138.74	1.06	361.99	162.52	1.10	415.16	187.78	0.54	468.23	236.44	0.70			

[a] Below Tg (440 K), the PVP sample was in the glassy state. As noted in footnote f of Table 10, for the PVP sample after being heated at 373 K for 30 min and then further heated at 473 K for 10 min, no impurity peaks were observed in the GPC-MALS measurement. Furthermore, heat treatment was performed at 520 K in the DSC cell prior to measurement. Considering that the weight loss between 520-550 K was 0.16 wt% (shown in Fig. 2) and that the weight loss includes the pyrolysis of PVP, the residual water content would be estimated as below 0.16 wt%.

[b] Temperature calibration of DSC was carried out to ± 0.1 K using onsets of the transition peaks for octane, water, indium and tin.

[c] C_P^{DSC} represents the experimental data measured by DSC at an atmospheric pressure of 100.25 ± kPa. The molar mass of the repeating unit of PVP is 111.1436 g mol^{-1}.

[d] U represents the relative expanded uncertainty (coverage factor: $k = 2$).

Table 14
Calculated heat capacities as a function of temperature for solid PVP.

T K	$C_V^{skeletal}$ [a] J K^{-1} mol^{-1}	C_V^{group} [b] J K^{-1} mol^{-1}	C_V^{cal} [c] J K^{-1} mol^{-1}	C_P^{cal} [d] J K^{-1} mol^{-1}	T K	$C_V^{skeletal}$ [a] J K^{-1} mol^{-1}	C_V^{group} [b] J K^{-1} mol^{-1}	C_V^{cal} [c] J K^{-1} mol^{-1}	C_P^{cal} [d] J K^{-1} mol^{-1}
0.1	9.0E-07	0.000	9.0E-07	9.0E-07	260	42.66	72.45	115.11	119.70
0.2	7.2E-06	0.000	7.2E-06	7.2E-06	270	43.11	75.99	119.10	124.04
0.3	2.4E-05	0.000	2.4E-05	2.4E-05	273.15	43.24	77.12	120.37	125.42
0.4	5.7E-05	0.000	5.7E-05	5.7E-05	280	43.52	79.61	123.13	128.43
0.5	1.1E-04	0.000	1.1E-04	1.1E-04	290	43.90	83.29	127.19	132.87
0.6	1.9E-04	0.000	1.9E-04	1.9E-04	298.15	44.18	86.33	130.51	136.51
0.7	3.1E-04	0.000	3.1E-04	3.1E-04	300	44.24	87.03	131.27	137.34
0.8	4.6E-04	0.000	4.6E-04	4.6E-04	310	44.56	90.81	135.36	141.84
0.9	6.5E-04	0.000	6.5E-04	6.5E-04	320	44.85	94.61	139.46	146.37
1	9.0E-04	0.000	9.0E-04	9.0E-04	330	45.12	98.44	143.56	150.90
1.2	1.6E-03	0.000	1.6E-03	1.6E-03	340	45.37	102.29	147.65	155.44
1.4	2.5E-03	0.000	2.5E-03	2.5E-03	350	45.60	106.13	151.73	159.98
1.6	3.7E-03	0.000	3.7E-03	3.7E-03	360	45.81	109.96	155.78	164.51
1.8	5.2E-03	0.000	5.2E-03	5.2E-03	370	46.01	113.79	159.80	169.02
2	7.2E-03	0.000	7.2E-03	7.2E-03	380	46.20	117.59	163.79	173.50
3	0.024	0.000	0.024	0.024	390	46.37	121.36	167.73	177.96
4	0.057	0.003	0.061	0.061	400	46.53	125.11	171.64	182.39
5	0.112	0.027	0.139	0.140	410	46.68	128.81	175.49	186.78
6	0.193	0.108	0.301	0.301	420	46.82	132.48	179.30	191.13
7	0.306	0.273	0.579	0.580	430	46.95	136.10	183.05	195.44
8	0.452	0.532	0.983	0.985	440	47.08	139.68	186.75	199.70
9	0.631	0.872	1.503	1.505	450	47.19	143.20	190.39	203.92
10	0.841	1.274	2.116	2.119	460	47.30	146.67	193.98	208.08
15	2.219	3.640	5.859	5.872	470	47.40	150.09	197.50	212.20
20	3.796	5.981	9.776	9.805	480	47.50	153.46	200.96	216.26
25	5.351	8.136	13.49	13.54	490	47.59	156.77	204.36	220.27
30	6.841	10.16	17.00	17.08	500	47.68	160.03	207.71	224.23
40	9.67	14.08	23.74	23.88	510	47.76	163.23	210.99	228.14
50	12.36	17.84	30.20	30.42	520	47.84	166.37	214.21	231.99
60	14.99	21.28	36.27	36.60	530	47.91	169.46	217.37	235.79
70	17.55	24.32	41.86	42.30	540	47.98	172.49	220.48	239.54
80	20.02	26.95	46.97	47.53	550	48.05	175.47	223.52	243.24
90	22.39	29.25	51.64	52.34	560	48.11	178.40	226.51	246.89
100	24.63	31.33	55.96	56.80	570	48.17	181.27	229.44	250.48
110	26.71	33.28	60.00	60.99	580	48.23	184.09	232.31	254.03
120	28.64	35.19	63.83	64.97	590	48.28	186.85	235.13	257.53
130	30.40	37.10	67.51	68.82	600	48.33	189.57	237.90	260.98
140	32.01	39.08	71.09	72.59	610	48.38	192.24	240.62	264.39
150	33.46	41.15	74.61	76.30	620	48.43	194.85	243.28	267.75
160	34.78	43.33	78.11	80.00	630	48.47	197.42	245.89	271.06
170	35.97	45.64	81.61	83.71	640	48.51	199.94	248.46	274.34
180	37.04	48.09	85.13	87.45	650	48.55	202.42	250.97	277.56
190	38.01	50.67	88.69	91.24	660	48.59	204.85	253.44	280.75
200	38.89	53.40	92.29	95.10	670	48.63	207.23	255.87	283.90
210	39.68	56.27	95.95	99.01	680	48.67	209.58	258.24	287.01
220	40.40	59.27	99.67	103.01	690	48.70	211.88	260.58	290.08
230	41.05	62.39	103.44	107.07	700	48.73	214.14	262.87	293.11
240	41.64	65.64	107.28	111.21	710	48.76	216.35	265.12	296.11
250	42.18	69.00	111.17	115.42	720	48.80	218.53	267.33	299.07

[a] Heat capacity at constant volume (C_V) based on the skeletal vibration contribution.
[b] C_V based on the group vibration contribution.
[c] C_V calculated from ($C_V^{skeletal} + C_v^{group}$).
[d] Heat capacity at constant pressure computed by substituting C_V^{cal} into Eq. (12).

Resources, Supervision, Writing – review & editing. **Motohiro Nakano:** Methodology, Data curation, Validation, Formal analysis, Investigation, Resources, Supervision, Writing – review & editing. **Yasuhiro Nakazawa:** Methodology, Data curation, Validation, Formal analysis, Investigation, Resources, Supervision, Writing – review & editing.

Declaration of Competing Interest

The authors declare that they have no known competing financial interests or personal relationships that could have appeared to influence the work reported in this paper.

Data availability

Data will be made available on request.

Acknowledgments

We would like to express our sincere gratitude to Prof. Marek Pyda and the late Prof. Bernhard Wunderlich for their valuable guidance and advice on the ATHAS data bank. We would also like to express our deepest appreciation to Ms. Rena Ota for the TG measurement and Mr. Norihiro Mochizuki for the GPC measurement.

Appendix

Supplementary information on the samples used in the experiment is given in Table 10 and heat capacity data measured using adiabatic calorimetry and DSC are provided in Tables 11–13. Furthermore, the calculated heat capacities of solid PVP are listed in Table 14.

References

[1] H. Tanzawa, S. Nagaoka, Y. Mori, H. Inagaki, K. Nosaka, K. Ishikiriyama, M. Todoki, Relationship between state of water around polymer chains in hydrogels and haemocompatibility, in: Proceedings of the 14th Symposium Medicine Polymer, 1985, pp. 30–31.

[2] A. Yamada-Nosaka, K. Ishikiriyama, M. Todoki, H. Tanzawa, 1H-NMR studies on water in methacrylate hydrogels. I, J. Appl. Polym. Sci. 39 (1990) 2443–2452, https://doi.org/10.1002/app.1990.070391117.

[3] M. Tanaka, A. Mochizuki, Clarification of the blood compatibility mechanism by controlling the water structure at the blood-poly(meth)acrylate interface, J. Biomater. Sci. Polym. Ed. 21 (2010) 1849–1863, https://doi.org/10.1163/092050610X517220.

[4] M. Tanaka, S. Kobayashi, D. Murakami, F. Aratsu, A. Kashiwazaki, T. Hoshiba, K. Fukushima, Design of polymeric biomaterials: the "intermediate water concept, Bull. Chem. Soc. Jpn. 92 (2019) 2043–2057, https://doi.org/10.1246/bcsj.20190274.

[5] M. Tanaka, S. Morita, T. Hayashi, Role of interfacial water in determining the interactions of proteins and cells with hydrated materials, Colloids Surf. B Biointerfaces 198 (2021), 111449, https://doi.org/10.1016/j.colsurfb.2020.111449.

[6] Y. Furushima, K. Ishikiriyama, Y. Ueno, H. Sugaya, Analysis of the state of water in polyvinylpyrrolidone aqueous solutions using DSC method, Thermochim. Acta 538 (2012) 43–47, https://doi.org/10.1016/j.tca.2012.03.010.

[7] B. Wunderlich, Thermal Analysis, Academic Press, Inc., 1990.

[8] G. Zhang, B. Wunderlich, A new method of fitting approximate vibrational spectra to heat capacities of solids with Tarasov functions, J. Therm. Anal. 47 (1996) 899–911, https://doi.org/10.1007/BF01979438.

[9] B. Wunderlich, The heat capacity of polymers, Thermochim. Acta 300 (1997) 43–65, https://doi.org/10.1016/s0040-6031(96)03126-7.

[10] B. Wunderlich, Thermal analysis of polymeric materials, Springer, Berlin Heidelberg, 2005, https://doi.org/10.1007/b137476.

[11] J. Pionteck, M. Pyda, Part 2: Thermodynamic Properties – pVT – Data and Thermal Properties, Subvolume A: Polymer Solids and Polymer Melts, Springer, 2014.

[12] M. Pyda, The Advanced THermal Analysis System (ATHAS) Databank – Polymer Thermodynamics, Springer Mater, 2014. https://materials.springer.com/.

[13] F. Franks, T. Wakabayashi, Heat capacities of undercooled aqueous solutions of polyvinylpyrrolidone, Z. Fur Phys. Chem. 155 (1987) 171–180, https://doi.org/10.1524/zpch.1987.155.Part_1_2.171.

[14] M. Pyda, Conformational contribution to the heat capacity of the starch and water system, J. Polym. Sci. Part B Polym. Phys. 39 (2001) 3038–3054, https://doi.org/10.1002/polb.10060.

[15] R. Pan, M. Varma-Nair, B. Wunderlich, A computation scheme to evaluate debye and tarasov equations for heat capacity computation without numerical integration, J. Therm. Anal. 36 (1990) 145–169, https://doi.org/10.1007/BF01912078.

[16] S. Lau, B. Wunderlich, Calculation of the heat capacity of linear macromolecules from theta-temperatures and group vibrations, J. Therm. Anal. 28 (1983) 59–85, https://doi.org/10.1007/BF02105280.

[17] M. Pyda, M. Bartkowiak, B. Wunderlich, Computation of heat capacities of solids using a general Tarasov equation, J. Therm. Anal. Calorim. 52 (1998) 631–656, https://doi.org/10.1023/A:1010188110516.

[18] K. Ishikiriyama, M. Pyda, G. Zhang, T. Forschner, J. Grebowicz, B. Wunderlich, Heat capacity of Poly-p-dioxanone, J. Macromol. Sci. Phys. 37 (1998) 27–44, https://doi.org/10.1080/00222349808220453.

[19] M. Nakagaki, S. Shimabayashi, Journal of the Chemical Society of Japan, J. Chem. Soc. Jpn. 92 (1971) 508–513, 10.1246/nikkashi1948.92.508.

[20] Y. Miyazaki, T. Matsuo, Thermal and dielectric properties of manganese squarate clathrate compound, Thermochim. Acta 163 (1990) 225–232, https://doi.org/10.1016/0040-6031(90)80401-J.

[21] NIST Chemistry WeBook, (SRD69), https://webbook.nist.gov/cgi/cbook.cgi?ID=C111659&Mask=4NIST.

[22] E. Gmelin, M.S. Sarge, Calibration of differential scanning calorimeters, Pure Appl. Chem. 67 (1995) 1789–1800, https://doi.org/10.1351/pac199567111789.

[23] H. Preston-Thomas, The International temperature scale of 1990 (ITS-90), Metrologia 27 (1990) 3–10, https://doi.org/10.1088/0026-1394/27/1/002.

[24] S. Rudtsch, Uncertainty of heat capacity measurements with differential scanning calorimeters, Thermochim. Acta 382 (2002) 17–25, https://doi.org/10.1016/S0040-6031(01)00730-4.

[25] T.G. Kulagina, B.V. Lebedev, Thermodynamic properties of poly-N-vinylpyrrolidone in the temperature range from 0 to 450 K, Zh. Fiz. Khim. 73 (1999) 800–805.

[26] P.R. Couchman, Thermodynamics and the compositional variation of glass transition temperatures, Macromolecules 20 (1987) 1712–1717. https://pubs.acs.org/doi/pdf/10.1021/ma00173a045.

[27] M. Sugisaki, H. Suga, S. Seki, Calorimetric study of the glassy state. IV. Heat capacities of glassy water and cubic ice, Bull. Chem. Soc. Jpn. 41 (1968) 2591–2599, https://doi.org/10.1246/bcsj.41.2591.

[28] Ozawa, T. ed., IEEJ (The Institute of Electrical Engineers of Japan) Technical Report, 529 (1995) 55–59, https://dl.ndl.go.jp/pid/3237353/1/1.

[29] T.G. Kulagina, B.V. Lebedev, Heat capacity and thermodynamic functions of N-vinylpyrrolidone at 0-330 K, Zh. Fiz. Khim. 71 (1997) 804–808.

[30] A. Xenopoulos, B. Wunderlich, Thermodynamic properties of liquid and semicrystalline linear aliphatic polyamides, J. Polym. Sci. Part B Polym. Phys. 28 (1990) 2271–2290, https://doi.org/10.1002/polb.1990.090281209.

[31] H. Suzuki, B. Wunderlich, Heat capacities of liquids linear aliphatic polyoxides, J. Polym. Sci. Part A-2, Polym. Phys. 23 (1985) 1671–1679, https://doi.org/10.1002/pol.1985.180230818.

[32] Y. Furushima, M. Nakada, H. Takahashi, K. Ishikiriyama, Study of melting and crystallization behavior of polyacrylonitrile using ultrafast differential scanning calorimetry, Polymer (Guildf) 55 (2014) 3075–3081, https://doi.org/10.1016/j.polymer.2014.05.015.

[33] N. Okui, Relationships between melting temperature, maximum crystallization temperature and glass transition temperature, Polymer1 31 (1990) 92–94, https://doi.org/10.1016/0032-3861(90)90355-3.

[34] J. Grebowicz, B. Wunderlich, S. Lau, The Thermal Properties of Polypropylene, J. Polym. Sci. Polym. Symp. 71 (1984) 19–37, https://doi.org/10.1002/polc.5070710106.

[35] M.W. Schmidt, K.K. Baldridge, J.A. Boatz, S.T. Elbert, M.S. Gordon, J.H. Jensen, S. Koseki, N. Matsunaga, K.A. Nguyen, S. Su, T.L. Windus, M. Dupuis, General atomic and molecular electronic structure system, J. Comput. Chem. 14 (1993) 1347–1363, https://doi.org/10.1002/jcc.540141112.

[36] M. Varma-Nair, R. Pan, B. Wunderlich, Heat capacities and entropies of linear, aliphatic polyesters, J. Polym. Sci. Part B Polym. Phys. 29 (1991) 1107–1115, https://doi.org/10.1002/polb.1991.090290909.

[37] A. Czerniecka-Kubicka, I. Zarzyka, J. Schliesser, B.F. Woodfield, M. Pyda, Vibrational heat capacity of Poly(N-isopropylacrylamide) this paper is dedicated in memory of Professor Bernhard Wunderlich, Polymer (Guildf) 63 (2015) 108–115, https://doi.org/10.1016/j.polymer.2015.02.051.

[38] S.E. Lapuk, M.A. Ponomareva, A.V. Galukhin, T.A. Mukhametzyanov, C. Schick, A. V. Gerasimov, Glass transition kinetics and physical aging of polyvinylpyrrolidones with different molecular masses, Macromolecules 55 (2022) 4516–4522, https://doi.org/10.1021/acs.macromol.2c00547.

[39] K. Ishikiriyama, Polymer informatics based on the quantitative structure-property relationship using a machine-learning framework for the physical properties of polymers in the ATHAS data bank, Thermochim. Acta 708 (2022), 179135, https://doi.org/10.1016/j.tca.2021.179135.